Picoplanktonic methane production in eutrophic surface waters

Sandy E. Tenorio[1, 2, 4], Laura Farías[1, 2, 3]

[1]Departamento de Oceanografía, Facultad de Ciencias Naturales y Oceanográficas, Universidad de Concepción, Concepción, 4070043, Chile.
[2]Centro de Ciencia del Clima y la Resiliencia (CR2), Chile.
[3]Instituto Milenio en Socio-ecología Costera (SECOS), Chile.
[4]Programa de Graduados en Oceanografía, Departamento de Oceanografía, Universidad de Concepción, Concepción, 4070043, Chile.

Correspondence to: Laura Farías (laura.farias@udec.cl)

Abstract. In the last decade, there have been several research articles on the methane paradox (aerobic CH4 production) first described in the 1960s. In this study, we present observations of CH4 supersaturation in the surface layer in the central Chile upwelling zone (36° S, 73° W) throughout two seasonal cycles (2018-2021). Additionally, CH4 cycling experiments were performed using plankton fractions (natural planktonic community, <150, <3 and <0.2 μm) in a seasonal phytoplankton succession. Our findings highlight the significant role of picoplankton (<3 μm) in CH4 production on the ocean surface, contrasting with the limited involvement of larger organisms (<150 μm). Incubations with methylated substrates such as methylphosphonic acid (MPn) and trimethylamine (TMA) stimulated CH4 production in the picoplankton fraction during both upwelling (austral spring-summer) and non-upwelling (winter) seasons, being particularly relevant in the later period when Synechococcus contributed with high relative abundance. Long-term microcosm experiments underscore the importance of heterotrophic bacteria and cyanobacteria in methylotrophic methanogenesis, enhancing CH4 regeneration, mediated by dissolved organic matter (DOM) recycling. In conclusion, picoplankton emerges as a key factor in both production and metabolization of methylated substrates, being responsible for maintaining CH4 supersaturation. These findings provide valuable insights into the biogeochemical processes driving CH4 dynamics in highly productive upwelling waters.

Key words: dissolved methane, oxic methane production, surface layer, picoplankton, coastal upwelling**.**

Key points:

1. Picoplankton (<3 μm) are identified as key players in CH_4 production in the ocean surface layer, in light and dark conditions, while larger organisms (<150 μm) do not significantly contribute to this process.

2. Methylated substrates, such as methylphosphonic acid (MPn) and trimethylamine (TMA), stimulate CH_4 production in the picoplankton fraction.

3. *Synechococcus* and MPn substrate could be important components for CH_4 generation during the non-upwelling season, while picoeucaryotes and TMA substrate are important during the onset of upwelling for CH_4 generation.

4. Picoplankton's role in methylotrophic methanogenesis is crucial in maintaining CH_4 supersaturation in the surface layer and contributing in part to CH_4 exchange with the atmosphere.

1 Introduction

Methane (CH_4) is the most abundant organic molecule on Earth and acts as a potent greenhouse gas, with a radiative power thirty times greater than CO_2 over 100 years, positively affecting the global heat balance (IPCC, 2021). Its short lifetime, about 10 years, makes it possible to take actions to mitigate climate change (Harmsen et al., 2020). In the ocean, physical and biogeochemical processes modulate CH_4 distribution in a complex manner, especially in the surface layer (Weber et al., 2019). Biogeochemically, CH_4 regeneration is governed by methanogenesis; conducted by methanogenic archaea in sediments and oxygen-deficient zones (Reeburgh, 2007), whereas methanotrophy, performed by methanotroph bacteria, consuming CH_4, slows its exchange with the atmosphere (Bates et al., 1996; Saunois et al., 2020).

Paradoxically, non-methanogenic processes produce CH_4 in oxygenated surface environments (Liu et al., 2022; Karl et al., 2008). These processes could be important sources of biogenic CH_4, maintaining well observed CH_4 supersaturations in the ocean surface (Lamontagne et al., 1973; Karl et al., 2008; Repeta et al., 2016), but not-well documented in global balances (Saunois et al., 2020). In the last decade, phytoplankton has been identified as an important nexus in CH_4 production in different marine ecosystems, linked to pathways such as demethylation via methylated compounds, which serve as substrates for aerobic CH_4 regeneration (Damm et al., 2010; Florez-Leiva et al., 2013; Lenhart et al., 2016; Karl et al., 2008; Sun et al., 2011).

Some of these compounds are produced/synthesized or exudated/degraded by diverse microbes such as *Nitrosopumilus maritimus*, which produces phosphonates like methylphosphonic acid (MPn) (Metcalf et al., 2012); while different phytoplanktonic size fractions contribute to sulphur derivatives like methionine (Lenhart et al., 2016), dimethylsulfoniopropionate (DMSP), and dimethyl sulfide (DMS) (Belviso et al., 1990; Stefels and Van Boekel, 1993) as well as trimethylamines (TMA) (Sun et al., 2019). These substrates serve as potential carbon sources for microorganisms generating CH_4, a process denominated methylotrophic methanogenesis.

Picoplankton (< 0.2 µm), the smallest plankton size excluding viruses, are abundant in the ocean surface (Johnson and Sieburth, 1979) and key to dissolved organic carbon (DOM) recycling (Pomeroy et al., 2007). The coupling between autotrophic (e.g., *Prochlorococcus sp.*, *Synechococcus sp.*) and heterotrophic picoplankton (e.g., Pelagibacter, SAR 11) could lead to CH_4 production from various C-1 compounds (Carpenter et al., 2012; Repeta et al., 2016; Sun et al., 2019). Furthermore, Cyanobacteria serve as a CH_4 source through H_2 production during N_2 fixation (Berg et al., 2014).

The concentration and composition (quality) of DOC play a crucial role in marine CH_4 biogeochemistry, as DOC is released, consumed, and transformed (Azam and Malfatti, 2007). Specifically, heterotrophic prokaryotes degrade up to 50% of the carbon fixed by primary producers (Azam et al., 1983), reintroducing it into higher trophic levels through the microbial loop (Azam et al., 1983; Pomeroy et al., 2007). Additionally, they remineralize nutrients and generate greenhouse gases, such as CH_4 (Dinasquet et al., 2018; Sun et al., 2011). This highlights the intricate pathways involved in the biological origin of CH_4. Several studies have indicated empirical correlations between pico- and microplankton (haptophytes, cryptophytes, and diatoms) biomass and CH_4 supersaturation (Bizic, 2021; Klintzsch et al., 2020; Lamontagne et al., 1973), suggesting a not

68 well-known mechanism linking photosynthesis with a methylated precursor (Bižić et al., 2020; Hartmann et al., 2020; Lenhart
69 et al., 2016; León-Palmero et al., 2020); however, since picoplankton are small in size and biomass, it is difficult to observe
70 this relationship. Understanding the interaction between plankton fractions and organic substrates is essential for
71 comprehending the biogeochemical dynamics of CH_4 in the upwelling waters of central Chile, and has broader implications
72 for marine ecosystems in general.

2 Material and methods

2.1 Water collection

75 Seawater was collected from the upwelling zone of central Chile (36° 0.802' S 73° 07.750' W) at the University of Concepcion
76 (Chile) time series station, ST18. Monthly samplings have been conducted aboard the RV Kay Kay II since 2002. Continuous
77 sampling with a CTD-O (SBE-19) instrument was performed to obtain temperature, salinity, and dissolved oxygen (DO)
78 profiles, whereas seawater samples using 10 L Niskin bottles at various depths (0, 5, 10, 20, 30, 50, 65, 80 m) were obtained
79 in triplicate for dissolved gas (oxygen and methane), nutrient and chlorophyll-a (Chl-a) analysis. Detailed methodologies can
80 be found in Farías et al. (2021). From March 2019 to June 2020, Dissolved Organic Carbon (DOC) samples were specifically
81 procured from depths of 5, 20, 50 and 80 m.

82 Furthermore, to investigate the role of different sized planktonic communities in CH_4 cycling, seawater was gathered at a depth
83 of 10 m, commonly associated with the Chl-a peak, as observed in studies such as Testa et al. (2018). These samples were
84 earmarked for experiments with size-fractionated planktonic communities. Large zooplankton (150 µm mesh sieve) were
85 excluded using the methodologies outlined by Sieburth et al. (1978), and the experiment included enrichment with organic
86 substrates like MPn and TMA. The experimental setup is outlined in Table 1 and includes two variations of negative controls:
87 1) sterile filtration using a 0.2 µm filter, a widely employed technique for microorganism removal (Hahn, 2004), and 2) $HgCl_2$
88 addition, ensuring complete biological inactivation. The positive control was considered to be the natural community (NC),
89 with the entire community present naturally. To maintain the integrity of the samples, the seawater was transported in light-
90 restricted black drums under controlled temperature conditions to the Marine Station Biology laboratory at Dichato (Fig. 1),
91 minimizing the potential for biological activity. This is a time series study, from 2018 until 2021, encompassing CH_4 cycling
92 experiments in different productivity phases.

Table 1. Summary of the experimental setup of short-term (GC vials) and long-term (microcosms) experiments with different treatments: NC: seawater with the natural plankton (control); <3 µm: picoplankton; <0.2 µm: femtoplankton (control +); <0.2 µm + $HgCl_2$: femtoplankton with $HgCl_2$ (control +) and CC: picoplankton concentrate; and the addition of methylated substrates (MPN: methyl phosphonic acid and TMA: trimethylamines). Different phases of the productivity period are: PI: Phase I; PII: Phase II; and PIII: Phase III.

Date	Type of experiment	Setup	Plankton size (μm)	Place	Time (h)	Productivity period
December 2018	GC vials	Plankton fractionation	CN, <3 and <0.2	Incubator	24	High (PI)
January 2019	GC vials	Plankton fractionation	CN, <3 and <0.2	Incubator	24	High (PI)
March 2019	GC vials	Add: MPn	<3	Incubator	24	Intermediate (PII)
May 2019	GC vials	Add: MPn and TMA	<3	Incubator	24	Basal (PIII)
April 2019	Microcosms	Add: MPn and TMA	CN, <3, and CC	Cold room	60	Intermediate (PII)
September 2019	Microcosms	Add: MPn and TMA	CN, <3, and CC	Cold room	60	High (PI)

99
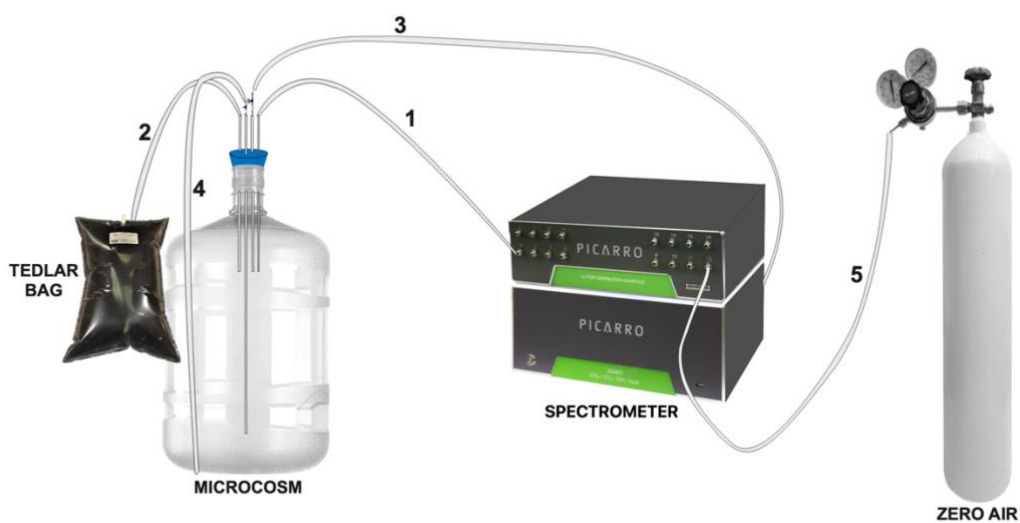
100
101 **Figure 1. Assembly of the microcosm for long-term experiments (10 L). Capillary 1 is connected directly to the spectrometer.**
102 **Capillary 2 is connected to a TEDLAR bag filled with N₂ (3L). Capillary 3 is removable and connected to the outlet of the**
103 **spectrometer. Capillary 4 is connected to a loose hose for water sampling and hose 5 is connected to zero air.**

Biogeosciences
Discussions
EGU
Open Access

104

2.2 Short-term experiments of CH_4 cycling by size-fractionated planktonic communities enriched with organic substrates.

The fractionation of planktonic communities based on size was conducted through a careful sequential filtration process, where 5 L of seawater was gently passed through a pre-filter of 150 μm nylon, followed by 3 μm Isopore, and 0.22 μm Millipore membranes, yielding two fractions: picoplankton (<3 μm), and femtoplankton (<0.2 μm) communities. NC was obtained directly without filtering, as is detailed in Table 1.

Prior to incubation, initial seawater sampling was taken for each treatment group, wherein triplicate measurements were taken of oxygen (125 mL), COD (60 mL), Chl-a (100 mL), and nutrients (15 mL). Subsequently, each size-fractionated sample was homogenized and swiftly transferred into 20 mL vials (108 in total, twenty-seven per treatment). These vials were immediately sealed using rubber and aluminium caps to prevent any potential atmospheric gas contamination. The incubation of these sample vials took place within an FOC 225E incubator, maintained at a temperature of 13 °C, and under a 12-hour photoperiod (24 hours). The illumination was calibrated to fall in a range of 11-11.5 μmol m^{-2} s^{-1} using blue and neutral density blank filters. At intervals of four hours, three vials from each treatment (Table 1) were withdrawn, and immediately poisoned with 50 μL of $HgCl_2$ and then, the vials were gently agitated to ensure homogenization. Gas chromatography was employed to analyze the CH_4 content of the vials.

In another set of experiments (Table 1), the picoplankton fraction was singled out to ascertain its capacity for metabolizing methylated substrates and subsequently cycling CH_4. This involved adding MPn and TMA to the samples. The final concentration of both substrates in these treatments was maintained at 1 μM, assuming that natural concentrations in the seawater were at trace levels. Thus, these could be considered as potential experiments (highly enriched). The experimental conditions remained consistent with those employed in the earlier experiment.

2.3 Long-term experiments of CH_4 cycling by size-fractionated planktonic communities enriched with organic substrates.

Nine microcosms were developed using a system of gas-tight polycarbonate bottles (13 L). Each microcosm contained 10L of seawater for treatment and 3L of headspace. They were equipped with a closed gas circuit and connected to a gas spectrometer analyzer capable of simultaneously and continuously measuring various gases, including CO_2, CH_4, N_2O, and humidity percentage. Each bottle featured a rubber cap equipped with four holes (as depicted in Fig. 1), housing a 5mm glass capillary within each hole. These capillaries were connected to gas-tight Teflon hoses. Specifically, the first capillary extended to the middle of the headspace (1) and was linked to an accessory (16-Port Distribution Manifold A0311) of the Picarro G-2308 spectrometer for Cavity Ring Spectroscopy System (CRDS), designed for the measurement of gases in equilibrium with the aqueous phase. The second capillary was suspended within the headspace (2) and connected to a Tedlar bag (3 L) filled with N_2. This arrangement aimed to prevent imbalance when drawing water samples from the microcosm. The third capillary, also

136 suspended in the headspace (3), was equipped with a 3-way cannula, and was connected to the air outlet of the Picarro G-2308

137 spectrometer, to facilitate the recirculation of air within the headspace. This system optimization aimed to mitigate excessive

138 headspace during spectrometer air sampling, preventing a gas-seawater phase imbalance. This hose (3) was adjustable and

139 replaced upon measuring gas concentrations in each microcosm. The fourth glass capillary was submerged in the seawater, 3

140 cm from the bottom (4). It was attached to a 3-way cannula, streamlining the sample extraction process.

141 In both April and September of 2019, a series of long-term microcosm experiments were conducted. These months were

142 strategically chosen: the first coinciding with the transition of phytoplankton composition to nano-picoplankton (the basal

143 productivity period), and the second with diatom blooms (larger phytoplankton dominance) (high productivity period), as

144 highlighted in studies by Anabalón et al. (2007), Cuevas et al. (2004), and González et al. (2007). The experiment encompassed

145 three distinct treatments, 1) Control without any methylated substrates added to natural communities (NC), picoplankton

146 community (< 3 µm) and concentrated picoplanktonic community (CC) 2) all treatments enriched with MPn 3) and all

147 treatments enriched with TMA (see Table 1).

148 The concentrated fraction of picoplankton (CC) was procured through tangential flow filtration via a 0.2 µm filter, following

149 a procedure developed by Giovannoni et al. (1990) for harvesting greater quantities of microbial biomass and using pre-

150 filtering steps as discussed earlier to concentrate only picoplankton (<3 µm). To discern whether the tangential flow filtering

151 was effective, the abundance of cyanobacteria, picoeukaryotes and heterotrophic bacteria was measured with flow cytometry.

152 The incubations were carried out within a controlled cold room environment, maintaining a temperature range of 12 to 13 °C,

153 with same illumination used in short periods over 60 hours. In the initial stages, each bottle was sealed and allowed to acclimate

154 for six hours in darkness. Following this stage, 1 mL of MPn (10 mM stock solution) and TMA (10 mM stock solution) were

155 introduced to each bottle, yielding a final concentration of 1 µM, matching the conditions established in prior experiments.

156 To prevent CH_4 residue contamination, a purge with Zero air was performed (as shown in Fig. 1, line 5), ensuring accurate

157 CH_4 concentration measurement within each microcosm, and establishing a baseline. Every four hours a cycle of CH_4

158 measurements was conducted continuously over 3 minutes, followed by a 6-minute hose cleaning (used for recirculation) with

159 Zero air before connecting to capillary 3 for subsequent measurement. It is important to note that the equipment absorbed 240

160 mL of air per minute of reading. Therefore, air recirculation within the microcosm, as previously mentioned, was essential.

161 Preceding the actual experiment, the concentrations of gases measured by the spectrometer were closely monitored for 30

162 minutes, confirming that the recirculation process did not impact the measured gas concentrations.

163 **2.4 Analytical analysis**

164 Once the CH_4 samples were taken, they were stored upside down, at room temperature and protected from light, and then

165 analyzed in the GC. CH_4 (discrete samples) was determined using the phase equilibrium method (McAuliffe, 1963). In this

166 procedure, each vial was carefully treated, with the addition of 5 mL of inert gas (helium), creating a headspace to facilitate

167 equilibrium between the aqueous and gas phases. Subsequently, the gas phase was measured in a gas chromatography

168 Shimadzu 17 equipped with a flame ionization detector (FID). A Restek RT QS-Bond column (30 m length, 0.53 mm inner

169 diameter, 20 μm film thickness) was employed, maintained at a temperature of 30 ℃ with a flow of 2.6 ml min^{-1}, using He as

170 an ultrapure gas carrier.

171 Five-point calibration curves (linear response of the detector) were made for each monthly sample set (treatment), using a gas

172 with a composition and concentration equivalent to that of the current atmosphere from NOAA (1863.4 ± 0.3 ppbv for CH_4)

173 (Bullister et al., 2016) as the primary standard, as well as three standard gas mixtures (Air Liquide, USA) and zero air (synthetic

174 air without CH_4 tracers). In each CH_4 sample set (every treatment), standards were added at the beginning, middle and end of

175 the measurements to corroborate the correct functioning of the detector. CH_4 measurements (triplicate) with a variation

176 coefficient greater than 10% were not considered.

177 To assess DO content, 125 mL glass flasks were used for sample collection in triplicate. These samples were immediately

178 fixed and analyzed within 6 hours of collection through the Winkler method (Carpenter, 1965). The analysis was conducted

179 using a Dosimat 665 instrument featuring an automatic photometric endpoint detector. The detection limit for this method

180 stood at 2 μmol L^{-1}. Nutrient samples were collected in triplicate using a 60 mL syringe and filtered through a 0.45 μm cellulose

181 acetate filter. The filtered content was held in 15 mL Falcon polyethylene bottles and stored at -20°C. Analysis of these nutrient

182 samples followed standard colorimetric techniques (Grasshoff et al. 1983) and was conducted using a SealAA3 segmented

183 flow auto-analyzer. This analyzer featured four distinct channels, each equipped with specific modules tailored for individual

184 nutrients.

185 To quantify Chl-a content, triplicate samples of 100 mL seawater were filtered using a GF/F filter and immediately stored at -

186 20°C. Analysis was performed according to the method outlined by Holm-Hansen et al. (1965). A Turner Designs 10AU

187 fluorometer was employed for measurement, and a standard pigment served as a reference (Sigma-Aldrich C6144-1MG). For

188 DOC assessment, samples were collected in triplicate using polyethylene bottles. Each 60 mL seawater sample was filtered

189 through a GF/F filter that had been pre-treated by heating at 450 °C for 4 hours. After filtration, the samples were acidified to

190 achieve a pH range of 2-3 and stored at -20 °C. These samples were analyzed via the infrared combustion method using a

191 Shimadzu Organic Carbon Analyzer (TOC-LCPH).

192 For picoplankton abundance, 3mL of water was fixed with a glutaraldehyde solution (1%) and promptly frozen (-80°C) in

193 liquid nitrogen for storage. Samples were analyzed with flow cytometry using an INFLUX, Cytopeia, equipped with five lasers

194 (355-457-488-532-638 nm). Sort gates were optimized based on the autofluorescence of each group. *Synechococcus sp.* were

195 identified based on their orange fluorescence (530/40 nm) using 488 nm blue and 532 nm green lasers, picoeukaryotes were

196 identified by their red fluorescence (692/40 nm) using 488 nm blue laser, and bacterioplankton were detected using a

197 combination of side scatter light (SSC) (related to cell size) versus green fluorescence (530/40 nm).

198 **2.5 Data analysis**

199 Dissolved CH_4 concentration was calculated using the solubility coefficient from Wiesenburg & Guinasso (1979). The

200 water column was divided into two layers according to density gradients: (1) surface layer (0 - 20 m) well mixed and (2)

201 subsurface layer (20 – 90m) from the base of the mixed layer to the bottom, around ~ 90 m (Farías et al., 2015), this was to

202 interpret the vertical and temporal variability of CH_4 variation.

203 Inventories of CH_4, Chl-a, nutrients, and nutrient ratios at the surface and subsurface layers were calculated through the

204 trapezoidal integration of concentrations of each variable at each layer, using a minimum of three depths per layer. The averages

205 were taken for DOC, because there were only two measurements taken per layer. The net CH_4 recycling rate (CH_4 accumulation

206 minus CH_4 consumption) in different fractions of the phytoplankton community was calculated through a linear regression of

207 CH_4 concentrations (Farías et al., 2009) during the incubation time (24 hours), separating the light cycles (12 hours of light

208 and 12 hours of darkness).

209 CH_4 saturation was calculated following Eq. (1):

210 $$Sat(\%) = \frac{[CH_4]_{in\ situ}}{[CH_4]_{eq}} \tag{1}$$

211 Where $[CH_4]_{eq}$ was calculated using the solubility coefficient from Wiesenburg & Guinasso (1979).

212 Monthly anomalies of CH_4, were estimated only in the surface layer, using the following Eq. (2)

213 $$Anomaly = \frac{xCH_4 - \bar{x}CH_4}{\sigma CH_4} \tag{2}$$

214 Where: xCH_4 is the discrete value at a certain depth (surface) and time (month), and $\bar{x}CH_4$ is the median value for the whole

215 (2018-2021) period at surface and σCH_4 is the standard deviation of this dataset.

216 CH_4 hot moments were defined as a ΔCH_4 three times higher than the average monthly disequilibrium anomaly ($\bar{x}\ \Delta CH_4$) at

217 each depth within the surface layer as Eq. (3).

218 $$\frac{\triangle CH_4}{\bar{x}_{\triangle CH_4}} > 3 \tag{3}$$

219 Where: ΔCH_4 is the disequilibrium of the gas at each depth and was estimated as Eq. (4):

220 $$\triangle CH_4 = [CH_4]_{in\ situ} - [CH_4]_{eq} \tag{4}$$

221 The daily CH_4 flux (F = μmol m^{-2} d^{-1}) across the air-sea interface was determined using the equation from Broecker and

222 Peng (1974), modified by Wanninkhof (1992) as follows Eq. (5):

223 $$F = K_w * (C_w - C^*) \tag{5}$$

224 Where: K_w (cm h^{-1}) is the transfer velocity from the surface water to the atmosphere, as a function of wind speed, temperature,

225 and salinity from the mixed layer depth (MLD), where wind speed were obtained from a meteorological station located at

226 Carriel Sur (http://www.meteochile.gob.cl/) and MLD was calculated using a potential density-based criterion of Kara et al.

227 (2003). C_w (nmol L^{-1}) is the mean CH_4 concentration in the mixed layer and C^* is the gas concentration in the mixed layer

228 expected to be in equilibrium with the atmosphere according to Wiesenburg & Guinasso (1979). Historical atmospheric

229 values were obtained from registers of gas hemispheric and global monthly means from the NOAA/ESRL program at NOAA

230 (http://www.esrl.noaa.gov). More details about the calculation of CH_4 fluxes are described in Farías et al. (2021).

Biogeosciences
Discussions

2.6 Statistical analysis

To determine significant differences between the upwelling and non-upwelling periods in both surface and subsurface layers, the non-parametric Mann-Whitney U test was used. To analyze the degree of relationship between oceanographic variables and the variability of CH_4 in the surface layer, Spearman correlations were used. In addition, the Kruskal-Wallis non-parametric statistical test was used to define significant differences between the concentrations produced by the different treatments. The statistically significant value was considered to be $p < 0.05$.

3 Results and discussion

3.1 Oceanographic features of wind-driven coastal upwelling in central Chile

The continental shelf off central Chile experiences wind-driven coastal upwelling, seasonally controlled by the migration of the South Pacific anticyclone (Strub et al., 1998). This process leads to alongshore equatorward winds during the summer-spring period, producing coastal upwelling (Sobarzo and Djurfeldt, 2004; Sobarzo et al., 2007). The area is influenced by Equatorial Subsurface Water (ESSW), which is nutrient rich and has low dissolved O_2 levels (less than 44 µM). The ESSW is carried southward by the Chile-Peru Counter Current (Strub et al. 1998). This subsurface water mass is a source of nutrients for the surface layer during coastal upwelling, but also interacts with sediments, delivering low O_2 concentrations and high organic matter content to the bottom water and sediments. This creates an environment conducive to anaerobic organic matter mineralization, which supports denitrification, sulphate reduction and methanogenesis (Ferderlman et al., 1997; Farías et al., 2004).

Thus, advection of CH_4-rich water from the subsurface and bottom layer, rather than in situ aerobic methanogenesis, has been described as the primary CH_4 source in the coastal upwelling regions. This mechanism has been observed in various eastern boundary upwelling systems, including California (Macías-Zamora, 2013; Sansone et al., 2001), Humboldt (Farías et al., 2021; Kelley and Jeffrey, 2002), Canary (Brown et al., 2014; Kock et al., 2008), and Benguela (Emeis et al., 2018; Monteiro et al., 2006; Morgan et al., 2019).

Our study reveals elevated CH_4 concentrations in the subsurface/bottom layer ranging from 0.43 to 78.72 nM (mean $\pm$ SD = 23.44 $\pm$ 15.38 nM, Fig. 2A), similar to the values found in long-term climatology (Farías et al., 2021). These elevated levels could be associated with the seasonal dynamics of organic matter mineralization under hypoxic to suboxic conditions during the favorable upwelling period (spring-summer); however, a similar subsurface/bottom CH_4 accumulation (p = 1.967) during the upwelling (22.52 $\pm$ 14.34) and non-upwelling (24.60 $\pm$ 16.65) periods was found (Fig. 2A).
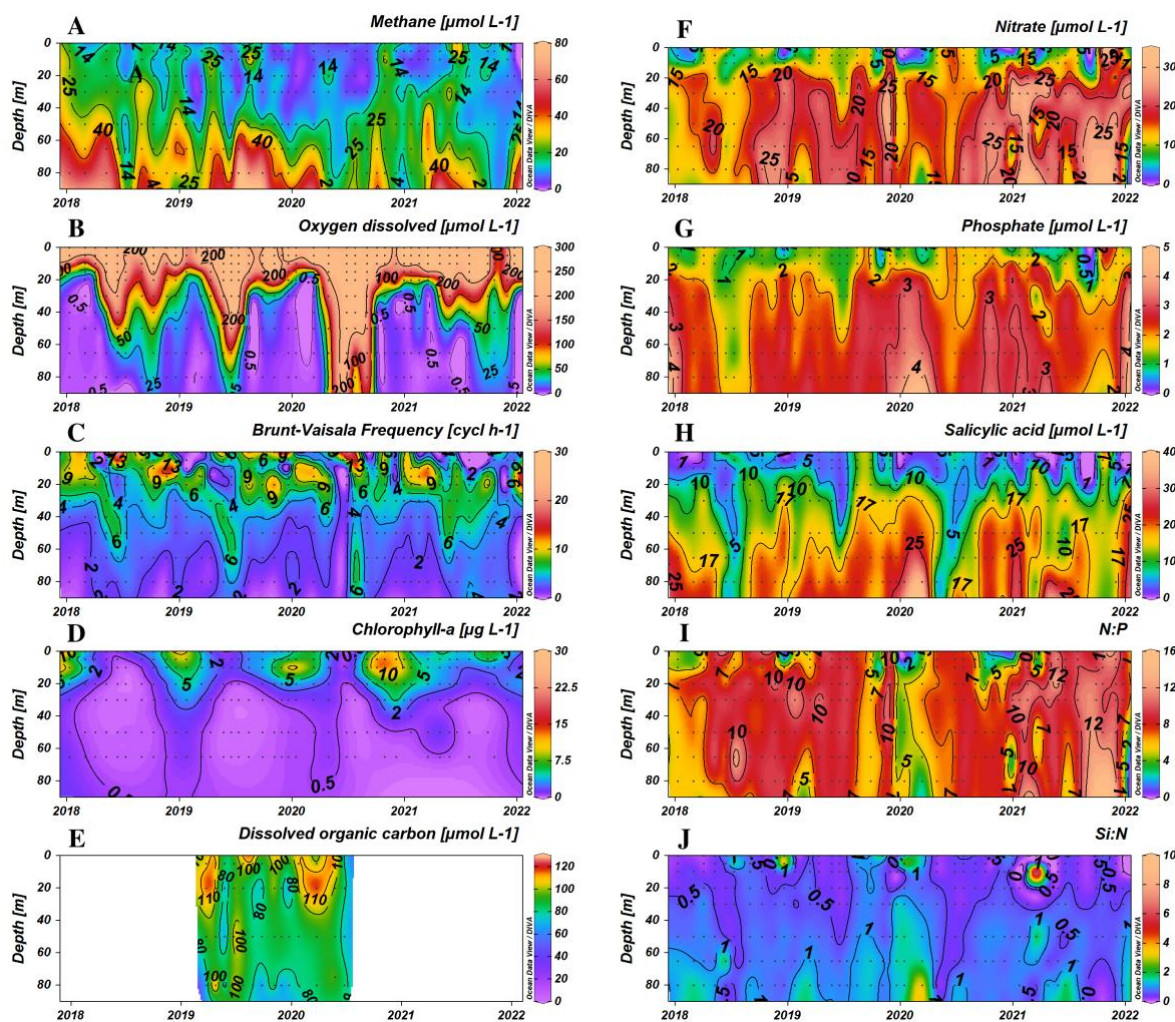
Figure 2. Time series of vertical distributions of A. Methane (μmol L^{-1}), B. Dissolved oxygen (μmol L^{-1}), C. Brunt-Vaisala Frequency (cycl h^{-1}), D. Chlorophyll-a (μg L^{-1}), E. Dissolved Organic Carbon (no Purgeable Organic Carbon - μM) from 2019 to 2020, F. Nitrate (μmol L^{-1}), G. Phosphate (μmol L^{-1}), H. Salicylic acid (μmol L^{-1}), N:P ratio and J. Si:N ratio. Sampling was made at ST18 from January 2018 to December 2021.

In the surface layer, CH_4 concentration exhibits a heterogeneous distribution, ranging from 0.140 to 41.72 nM (mean $\pm$ SD = 11.70 $\pm$ 7.79 nM). Again, there are no differences in CH_4 levels between non- and upwelling seasons (p = 1.654). Indeed, within the mixed layer depth (20 m), during short periods (months), hot moments (local accumulations) of high CH_4 levels ranging from 10.17 (390 % saturation) to 41.72 (1650 % saturation) are present indistinctly throughout the sampling period (Fig. S1). Furthermore, the hot moments consistently occur under oxygenated conditions ($O_2 > 200$ μmol L^{-1}) (Fig. 2B) and eutrophic conditions (Fig. 2D). Sometimes they do not appear to be associated with vertical advection of CH_4-rich bottom waters and are present during both coastal upwelling and non-upwelling periods (Fig 2A and B).

10

272   This raises the question if they could be associated with local microbial processes on the surface or from the well-known

273   vertical advection resulting from the upwelling process (Brown et al., 2014; Capelle and Tortell, 2016; Kock et al.,

274   2008; Farías et al., 2021). Furthermore, the fact that no distinct seasonal difference in CH_4 concentration in surface water

275   may also suggest a lateral advection from the Itata river that can discharge CH_4 (Bello, 2016), DOC (Vargas et al., 2016) and

276   chromophoric DOM (CDOM) (Rain-Franco et al., 2019), which would also stimulate CH_4 regeneration via photooxidation

277   (Li et al., 2020; Zhang and Xie, 2015).

278   Therefore, we assume that a portion of CH_4 exchanged with the atmosphere, ranged from 3.35 to 23.42 µmol m^{-2} d^{-1} (mean ±

279   SD = 10.10 ± 5.77 µmol m^{-2} d^{-1}), originates from the surface layer, based on recent reports on in situ aerobic methanogenesis

280   linked to the growth and metabolisms of microalgae (Cerbin et al., 2022; Günthel et al., 2020; Hartmann et al.,

281   2020; Lenhart et al., 2016; Del Valle and Karl, 2014; Zhao et al., 2022; Klintzsch et al., 2019) and bacteria

282   (Repeta et al., 2016; Metcalf et al., 2012; Sun et al., 2019). This production has been suggested to be an important source of

283   CH_4 fluxes in various aquatic systems, such as stratified lakes (Bižić-Ionescu et al., 2018; Donis et al., 2017; Fazi et al., 2021;

284   Grossart et al., 2011; Günthel et al., 2019, 2020; Tang et al., 2016; Wang et al., 2018) and in open oligotrophic oceans (Damm

285   et al., 2010; Karl et al., 2008; Repeta et al., 2016; Sosa et al., 2020; Ye et al., 2020), and could be the case of our study area,

286   particularly during the stratified period (winter) due to freshwater discharge.

287   It becomes apparent that *in situ* aerobic methanogenesis could play a significant role in driving CH_4 fluxes in coastal upwelling

288   off central Chile. So far, we know that CH_4 is regenerated in the surface layer through DMS (Florez-Leiva et al., 2013), where

289   several potential CH_4 sources might be active; but further research is needed to better understand the specific mechanisms and

290   the relative contributions of different microorganisms to overall CH_4 production in this dynamic marine environment.

291   **3.2 Biological productivity and other biogeochemical indicators**

292   Considering that upwelling systems have high levels of primary production and concomitant high organic matter cycling; it is

293   pertinent to investigate the extent to which the regenerated CH_4 is produced in the surface layer. Interestingly, while Chl-a

294   levels peak (mean ± SD = 6.60 ± 5.98 µg L^{-1}) in spring and early summer, basal levels of this pigment (mean ± SD = 0.09 ±

295   7.33 µg L^{-1}) remain high throughout the year (Morales and Anabalón, 2012; Testa et al., 2018). Curiously, the

296   accumulation of surface CH_4 does not necessarily coincide with high Chl-a levels (Fig 2D).

297   Based on productivity, biomass, and a shift in the composition of phytoplankton (phytoplankton succession), along with other

298   biophysical variables, the annual cycle of biological productivity has been separated into three distinct periods (Testa et al.,

299   2018): September to January, with high productivity and Chl-a biomass dominated by microplankton such as large diatoms,

300   tintinids, and dinoflagellates; February to April with intermediate productivity, characterized by a shift in plankton composition

301   and biomass from larger to smaller organisms as flagellates; and May to August, with basal level productivity and relatively

302   low Chl-a biomass. The latter (autumn-winter) is impacted by nutrient input from continental runoff and rivers with a

303 prevalence of picoplankton (e.g., *Synechococcus*) including small flagellates and ciliates. Therefore, factors such as
304 mixing/stratification (Fig. 2C) and a difference in nutrient contents and Si:N ratio (Fig. 2J) among phases (Table 2), due to
305 differential nutrient consumption or input from other sources, promote a shift in phytoplankton composition, from large
306 microorganisms during upwelling periods, to pico- and nanoplankton, such as small cyanobacteria (*Synechococus*) and small
307 ciliates, during non-upwelling periods (Anabalón et al., 2007; Collado-Fabbri et al., 2011; (Jacob et al., 2018),)(Jacob et al.,
308 2018). This cycle provides insight into the dynamics of primary productivity and CH_4 regeneration.

309

310 **Table 2. Average annual cycle of biochemical variables in each productivity period (mean ± SD) from 2018 to 2021, showing the**
311 **average chlorophyll (µg L^{-1}) concentration in each period and inventories of methane (µmol m^{-2}), chlorophyll-a (mg m^{-2}), DOC (µmol**
312 **m^{-2}), nitrate (µmol m^{-2}), phosphate (µmol m^{-2}), silicate (µmol m^{-2}), N:P and Si:N ratios in both surface (SL) and subsurface (SSL)**
313 **layers. Number of hot moments in each period are counted.**

Variable	Layer	Productivity periods		
		High **Phase I** **(spring-summer)**	**Intermediate – Phase II** **(summer-autumn)**	**Basal** **Phase III** **(autumn-winter)**
Chl-a	SL	6.60 ± 5.98	3.23 ± 2.87	1.36 ± 1.91
CH_4	SL	265.59 ± 58.36	162.35 ± 21.44	240.54 ± 78.97
	SSL	1315.07 ± 173.69	1012.86 ± 163.23	1275.17 ± 286.38
Chl-a	SL	154.4 ± 102.31	51.32 ± 31.02	26.19 ± 21.17
DOC	SL	114.44 ± 53.94	112.88 ± 8.36	92.41 ± 11.27
	SSL	100.35 ± 46.51	96.97 ± 23.78	86.12 ± 8.95
NO_3^-	SL	260.61 ± 96.25	208.67 ± 49.51	224.65 ± 13.44
	SSL	1274.41 ± 344.24	1033.51 ± 38.5	987.6 ± 113.58
PO_4^{-3}	SL	38.08 ± 10.35	30.29 ± 3.51	28.16 ± 2.99
	SSL	170.22 ± 34.07	137.05 ± 21.57	119.38 ± 11.73
$Si(OH)_4$	SL	131.75 ± 47.07	91.65 ± 38.68	111.24 ± 37.9
	SSL	1065.32 ± 206.98	811.2 ± 225.51	678.07 ± 168.68
N:P	SL	7.69 ± 2.57	7.59 ± 2.44	8.48 ± 0.55
	SSL	9.28 ± 2.52	8.24 ± 0.92	8.46 ± 0.84
Si:N	SL	0.67 ± 0.1	0.69 ± 0.73	0.49 ± 0.15
	SSL	1.04 ± 0.08	1.01 ± 0.26	0.74 ± 0.11
Hot moments	SL	19	9	15

314

315 Table 2 presents Chl-a levels along with inventories of CH_4, Chl-a, DOC, NO_3^-, PO_4^{-3}, $S(OH)_4$ and mean inorganic nutrient

316 ratios (N:P and Si:N) in each period. In contrast to CH_4, Chl-a exhibits a marked and expected seasonal cycle, with integrated

317 levels decreasing from spring to winter (Table 2). Hence, there could be a wide range in the composition of the phytoplankton

318 species involved in CH_4 cycling (Klintzsch et al., 2019; Günthel et al., 2020; Klintzsch et al., 2023). Recently, Klintzsch et al.

319 (2023) identified the carbon isotope fingerprint of CH_4 released from six widespread marine phytoplankton species, three

320 haptophyte algae and three cyanobacteria, incubated under laboratory conditions. They were clearly distinguished from CH_4

321 produced by methanogenic archaea, suggesting that algal and cyanobacterial populations may contribute substantially to CH_4

322 formation observed in the surface mixed layer of oceans and lakes.

323 Nutrient concentrations in the surface layer are subject to strong seasonal variability (Fig 2F, G and H) due to the advection of

324 nutrient-rich upwelled water, as well as biological assimilation in surface waters. Therefore, NO_3^- levels among upwelling and

325 non-upwelling period are significantly different (p<0,05), and a similar trend is observed for PO_4^{-3} and $Si(OH)_4$. Remarkably,

326 the inorganic N:P ratio, ranging from 0.15 to 15.01, are generally less than expected (Redfield stoichiometry). This is due to

327 the influence of Oxygen Minimum Zone (OMZ) (associated with ESSW), which is laterally and vertically advected to the

328 surface, indicating denitrified waters (Fernandez et al., 2015) and local denitrification (Silva et al, 2009; Farías et al., 2004).

329 Nutrients inventories show significant differences among the different productivity periods, with elevated levels in the

330 subsurface layer (Table 2). However, at the surface, $Si(OH)_4$ and the Si:N ratio only slightly increase from basal to high

331 productivity periods (Table 2), while the N:P ratio is higher in the basal productivity period. Moreover, during basal

332 productivity period, the increase of $Si(OH)_4$ is likely due to the freshwater discharge during the winter. This indicates that at

333 the beginning of upwelling (high productivity), when the water column begins to stratify (Fig. 2C) and there is a higher

334 predominance of Si (Si:N ratio) coming from the advection of cold and nutrient -rich water, the growth of large diatoms is

335 promoted (Morales and Anabalón, 2012; Anabalón et al., 2007), which, to a certain extent, results in the depletion

336 of this nutrient (Table 2). Whereas during the non-upwelling period, when the water column begins to mix (Fig. 2C) and the

337 nutrient regeneration rate change, the N:P ratio increases in basal productivity period, which leads to a predominance of

338 nitrogen-fixing organisms (cyanobacteria) and small ciliates (Anabalón et al., 2007; Collado-Fabbri et al., 2011).

339 High DOC concentrations, typical of highly productive coastal zones (Igarza et al., 2019; Vargas et al., 2013) are found in the

340 study area, ranging from 58.79 to 128.63μM (mean ± SD = 90.37 ± 17.05) and peaking at the surface during late summer and

341 early fall, with low values in subsurface layers (Fig 2E). At the surface, mean DOC inventory decreases between Phase I and

342 Phase III (Table 2), which suggests an increase in picoplanktonic abundance and activity in Phase III (Collado-Fabbri et al.,

343 2011) that allows a high DOC accumulation (Fig 2E) (Herndl and Malacic, 1987). In this period, significant DOC

344 accumulation could be ascribed to a DOC generation greater than its respective heterotrophic bacterial consumption (Hansell

345 and Orellana, 2021), or it may consist of refractory DOC that is difficult to degrade (Bauer and Druffel, 1998).

346 On the other hand, several hot moments (Fig. S1) are identified in different phases of productivity and phytoplankton

347 succession (Collado-Fabbri et al., 2011; Aldunate et al., 2018; Anabalón et al., 2007), even at different nutrients ratios and

348 DOC concentrations (Table 2), indicating that the factors favoring their occurrence are not entirely clear. Furthermore, we

349 found no significant correlation among biochemical variables at the surface (Fig. S2), suggesting that the interactions between

350 these variables are complex and not easily explained by simple linear relationships.

351 This complexity poses a challenge to understanding the dynamics of CH_4 in the studied system. To gain a deeper understanding

352 of CH_4 dynamics, short-term and long-term CH_4 cycling experiments have been conducted, focusing on size-fractioned

353 planktonic communities along with organic substrates. This approach makes it possible to explore and uncover the specific

354 interactions and substrates that may favor CH_4 production. By focusing on the size fractions of planktonic communities, the

355 contributions of diverse groups to CH_4 regeneration, such as phototrophic (primary producers like microalgae) and

356 heterotrophic assemblage's communities, could be assessed.

357 **3.3 Short-term CH_4 cycling by size-fractioned planktonic communities.**

358 The time course of CH_4 accumulation/depletion in fractioned plankton experiments with daily incubations (12 hours of light

359 and 12 hours of darkness) is shown in Fig. 3. The first experiments were conducted in December 2018 (Fig. 3A) and January

360 2019 (Fig. 3B), corresponding to a period of high productivity or phase I (Table S1), and coinciding with strong vertical

361 advection. Surface water exhibits cooling (~12 - 13 °C) and elevated CH_4 levels (9.44 – 17.09 nM), indicative of an active

362 upwelling period (Farías et al., 2021), aligning with other indicators of coastal upwelling (Aguirre et al., 2021).

363
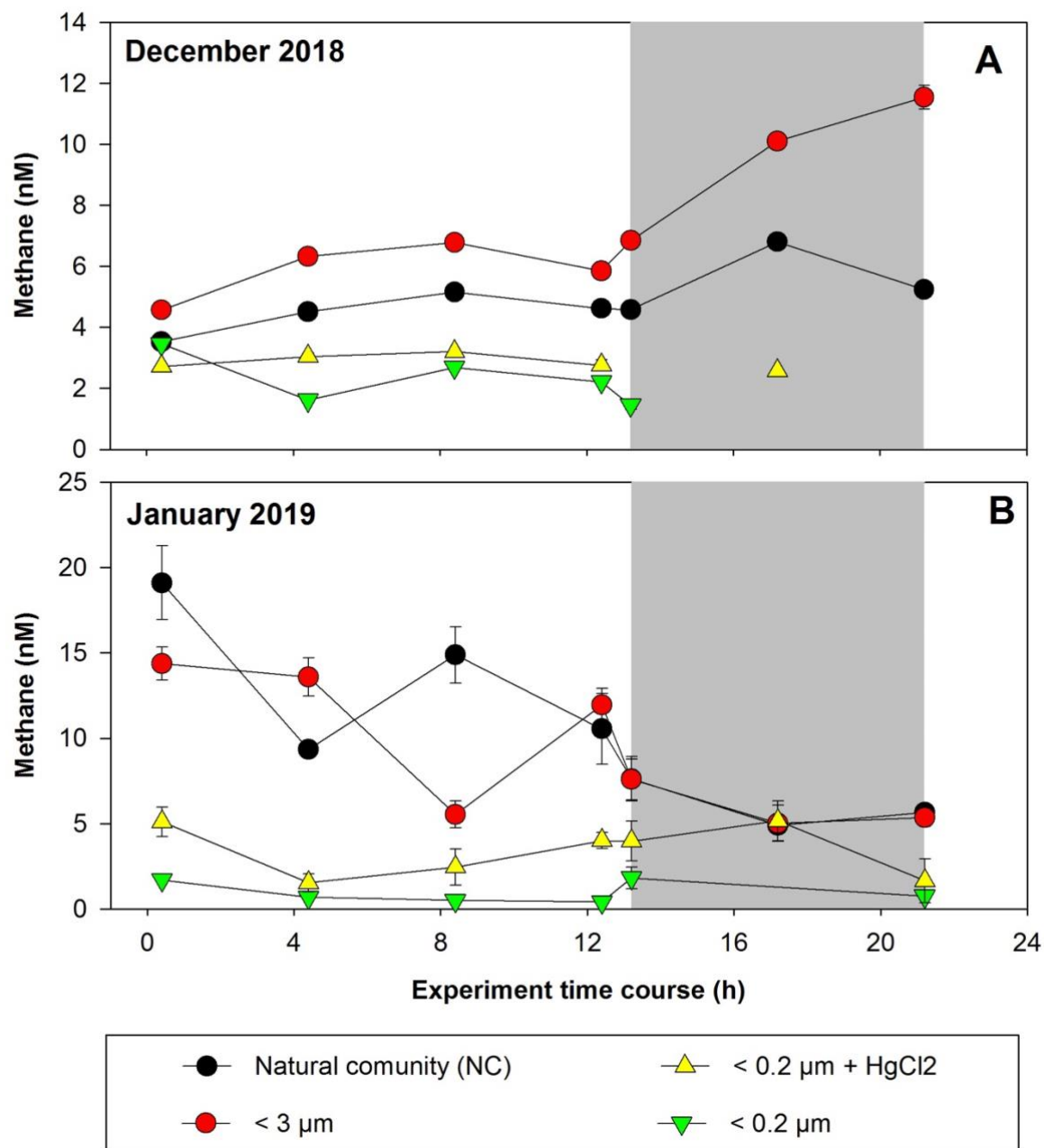
Figure 3. Time courses of dissolved methane concentration (nM) during incubations with fractionated plankton experiments (NC: natural community; <3 μm: bacterioplankton and <0,2 μm: femtoplankton. A. December 2018 and B. January 2019. Photoperiod is represented in white (light) and gray (dark). Error bars represent standard deviation of triplicate samples, when error bars are not visible, they are within the area of the symbol.

370 In the treatments involving fractions <0.2 μm and <0.2 μm + $HgCl_2$, which serve as negative controls, CH_4 concentration kept

371 almost constant during incubation, with concentrations below 2.32 nM (Fig. 3A) and 5.51 nM (Fig. 3B). This proves that CH_4

372 production is entirely biological (Table S2). Although abiotic CH_4 production via photooxidation of CDOM has been

373 demonstrated under oxygenated conditions (Li et al., 2020; Zhang and Xie, 2015), our experiments indicated that

374 abiotic processes, such as DOM photochemical reactions (Mopper et al., 2015), did not take place. However, this process may

375 contribute to the DOM pool to be photo oxidized, producing CH_4 at shallower depths (<10 m) (Li et al., 2020; Zhang &

376 Xie, 2015).

377 In December, CH_4 concentrations in the NC (positive control) and <3 μm fractions experienced slight increases under light

378 conditions (Fig. 3A, Table S2). However, during darkness, the net CH_4 accumulation was significantly higher in the <3 μm

379 fraction (p=0.03; Table S2). Picoplankton includes autotrophic and heterotrophic unicellular organisms in the size range of 0.2

380 to 2 μm. The autotrophic organisms include cyanobacteria (*Prochlorococcus* and *Synechococcus*) and diverse picoeukaryotes

381 larger than 1 μm (Worden, 2006), while the heterotrophic are primarily prokaryotes, with bacteria overwhelmingly dominating

382 over archaea in the upper layers (Smith et al., 2013). This fraction (<3 μm) hosts several coexisting metabolic groups,

383 dependent on or subsidized by different energy sources such as sunlight, DOM, or even a combination of the two

384 (mixotrophy).All together they are critical for the functioning of the microbial food web mainly responsible for DOC cycling

385 (Muñoz-Marín et al., 2020; Raven, 1998; Azam et al., 1983; Reintjes et al., 2020) and its derivative compounds (including

386 CH_4).

387 In January, the incubations displayed a distinctly different behavior, with CH_4 levels decreasing over incubation time in both

388 the NC and <3 μm fractions for both photoperiods (Fig. 3B), although the rate of consumption was lower in the dark (Table

389 S2). These differences suggest that the structure/composition of the microbial community during the high productivity period,

390 as well as the quantity and quality of DOC and nutrient concentrations and their ratios (Allen et al., 2012; Sarmiento et al.,

391 2013; Spilling et al., 2019; Sarmiento et al., 2013), may control CH_4 recycling. Indeed, the environmental conditions during

392 sampling differed (Table S1); although both months were oxygenated, both varied in Chl-a and nutrient levels, including CH_4.

393 In 2018, December marked the beginning of the upwelling, with the oxycline moving upward at 20 m (Fig. 2B), while in

394 January, the upwelling (vertical advection) was at its strongest (Fig. 2C; Table S1).

395 When the NC and even the <150 μm fraction treatments (data not shown) are compared with the <3 μm fraction, significant

396 differences in CH_4 recycling rates are found (p < 0.05), especially in darkness (Table S2). The highest recycling rates occur in

397 the <3 μm fraction, indicating that larger microorganisms do not affect the net CH_4 accumulation/consumption (Table S2),

398 and emphasizing the importance of the microbial loop (Azam et al., 1983) in CH_4 recycling. Additionally, the observed

399 differences between photoperiods in both fractions could suggest coupling mechanisms between autotrophic phytoplankton

400 and heterotrophic bacterioplankton communities (León-Palmero et al., 2020; Morán et al., 2002; Repeta et al., 2016). Here,

401 DOC accumulated in light conditions could be rapidly utilized by bacterioplankton in dark conditions (Hartmann et al., 2020;

402 Thornton, 2014), leading to high CH_4 concentrations.

403 CH$_4$ consumption by methanotrophs should be considered (Mao et al., 2022), since aerobic CH$_4$ oxidation can reduce the CH$_4$

404 accumulation rate (net production vs. consumption) by as much as half (Florez-Leiva et al., 2013). It is known that

405 methanotrophs are inhibited in light conditions (Dumestre et al. 1999; Morana et al., 2020), thus CH$_4$ accumulation should be

406 higher in this condition. However, this contrasts with our results (light/dark conditions), meaning that both methanotrophy and

407 methylotrophy are very dynamic and complex, making it difficult to decipher in a daily cycle.

3.4 Short-term CH$_4$ cycling experiment from picoplankton amended with organic substrates.

409 The picoplankton showed the highest rate of CH$_4$ accumulation, prompting its selection to be assessed for its potential for

410 methylotrophic methanogenesis through the addition of methylated substrates (MPn and TMA) in a daily cycle. Both MPn

411 and TMA are dissolved methylated compounds known to stimulate CH$_4$ production because they have a methyl radical (-CH$_3$),

412 a potential precursor for CH$_4$ formation in oxygenated environments (Karl et al., 2008; Repeta et al., 2016).

413 These compounds are ubiquitous in various ecosystems (Lohrer et al., 2020; Sun et al., 2019), yet they have distinct metabolic

414 origins. While MPn originates from Arquea *Nitrosopumilus maritimus* (Metcalf et al., 2012) and is found at very low

415 concentrations (~0.01 μM, close to its analytical detection limit), likely due to rapid microbial turnover (Karl et al. 2008;

416 Martínez et al. 2013; Urata et al. 2022), TMA exhibits a wide concentration range in the ocean, from nM levels in the open

417 ocean to μM levels in sediments and near the coast (Sun et al., 2019). Environmental TMA concentrations could be higher,

418 particularly in upwelling events that bring TMA from bottom waters to the surface (Gibb et al., 1999; Sun et al., 2019). In this

419 context, the amendments performed for each substrate, 100-fold for MPn and 1000-fold for TMA, have potential for

420 experimentation.

421 It is important to note that amended experiments were conducted in Phase II (March 2019) and phase III (May 2019), periods

422 of change in phytoplankton succession (composition), biomass and abundance (Testa et al., 2018). In winter, the relative

423 abundance of picoplankton with respect to microplankton (particularly the presence of *Synechococcus* and nitrifying archaea*)*

424 increases significantly, especially photosynthetic picoeukaryotes (Collado-Fabbri et al., 2011).

425 The time course CH$_4$ accumulation during incubations is illustrated in Fig. 4. The highest CH$_4$ accumulation was observed in

426 the MPn-amended treatment, particularly under dark conditions in May (Phase III) (Fig. 4B; Table S1). Interestingly, in both

427 periods, the <3 μm + MPn treatment exhibited contrasting patterns under dark conditions (Fig. 4A and 4B), decreasing in

428 Phase II and increasing in Phase III, suggesting the importance of microbial composition. During winter, a higher DOC

429 concentration was observed (Fig 2E), which may lead to higher bacterial and archaeal activity that could be metabolizing

430 DOC, including MPn under dark conditions.

431
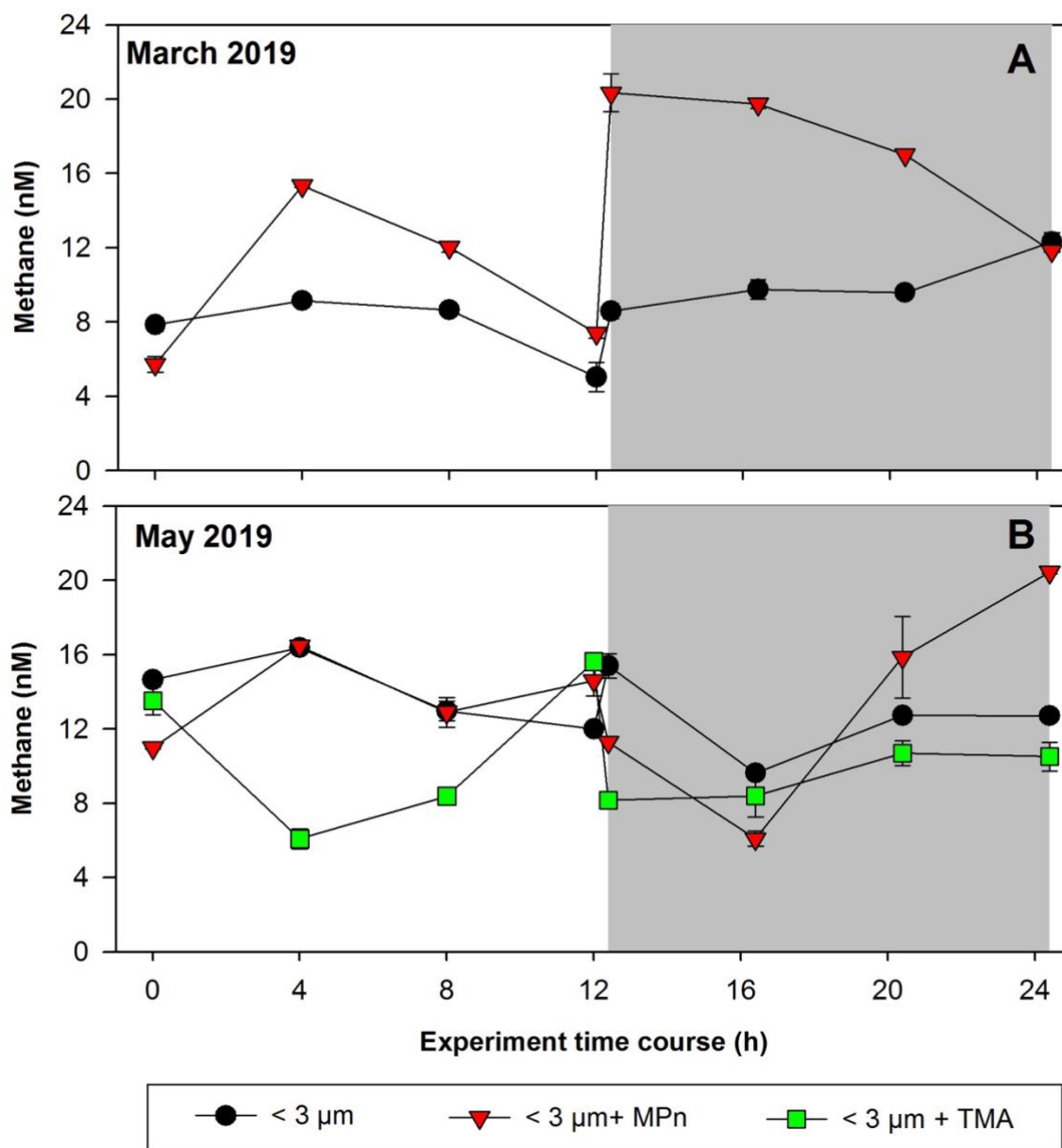
Figure 4. Time courses of dissolved methane concentration (nM) during incubations with the addition of methylated substrates (MPn: methyl phosphonic acid and TMA: trimethylamine) performed with bacterioplankton (<3 μm) and bacterioplankton concentrate (CC). A. March 2019 and B. May 2019. Photoperiod is represented in white (light) and gray (dark). Error bars represent standard deviation of triplicate samples, when error bars are not visible, they are within the area of the symbol.

438 Conversely, the TMA treatment did not result in any CH_4 accumulation. In fact, CH_4 accumulation in this treatment was lower
439 compared to the control and MPn treatments (Fig. 4B), contrary to expectations in a nitrogen-limited ecosystem. Indeed, in
440 the study area inorganic nutrient N:P ratios are consistently below the Redfield ratio of 16 (Redfield et al., 1963), in both
441 surface (mean ± SD: 7.354 ± 2.947) and subsurface (mean ± SD: 8.217 ± 3.443) layers. This N deficit is primarily influenced
442 by the lateral and vertical advection of denitrified water from equatorial origin (ESSW) transported poleward by the Peru-
443 Chile undercurrent (Fernandez et al., 2015; Fernandez & Farías, 2012; Silva et al., 2009), along with a local
444 dissimilative NO_3^- reduction during anaerobic organic matter mineralization (Farías et al., 2004) and possibly PO_4^{-3} release
445 from anoxic sediments (Holmkvist et al., 2010).

446 While TMA can be metabolized by marine bacteria (Lidbury et al., 2015; Bižić-Ionescu et al., 2018), the lower CH_4 production
447 in this treatment suggests a different outcome. In contrast, heterotrophic picoplankton might metabolize MPn and produce
448 CH_4, showing *in situ* methanogenesis via the carbon-phosphorus (C-P) lyase pathway (Karl et al., 2008). Although this
449 pathway has primarily been described for PO_4^{-3}-limited environments like gyres, the possibility of its occurrence in upwelling
450 areas with PO_4^{-3} excess cannot be dismissed, although the rates might be lower (Bižić-Ionescu et al., 2018).

451 **3.5 Long-term CH_4 cycling from concentrated picoplankton amended with organic substrates.**

452 Aiming for comprehensive insights, our study encompassed long-term microcosm experiments strategically performed during
453 two (of three) distinct phases of productivity as was described (Testa et al., 2018). The intermediate productivity phase (Phase
454 II or late summer - autumn time) was characterized by a notable relative prevalence of autotrophic cyanobacteria
455 (*Synechococcus*). In contrast, the high productivity period (Phase I or early spring time) (Fig. S3A and D) was marked by a
456 prevalence of diatoms (Fig. S3B and E), while heterotrophic bacterioplankton exhibited almost constant presence in both
457 periods (Fig. S3C and F). These temporal distributions align with well documented patterns in our study area, where light,
458 oxygen, temperature, and nutrient levels drove the seasonal and vertical segregation of specific cyanobacteria, picoeukaryotes
459 and heterotrophic bacterioplankton, which represent the <3 µm fraction in this study (Aldunate et al., 2018; Collado-Fabbri et
460 al., 2011; De La Iglesia et al., 2020; Molina et al., 2020).

461 Briefly, Flavobacteraceae, SAR11 subclade IA (*Candidatus Pelagibacter* ubique-associated), SAR11 subclade 1b,
462 gammaproteobacterial clades, and SAR86 are prevalent during upwelling seasons, while during non-upwelling seasons or
463 phase III, SAR11 subclade II, Marine Actinobacteria, and unclassified Alphaproteobacteria dominated (Aldunate et al., 2018).
464 Additionally, photosynthetic picoplankton eukaryotes related to Mamiellophyceae (Bathycoccus, Micromonas, and
465 Ostreococcus) were predominantly observed with high significance in the surface layer during the transition period (Collado-
466 Fabbri et al., 2011; De La Iglesia et al., 2020), whereas heterotrophic bacteria abundance ranging from 0.23 to 6.50 x10^6 cell
467 mL^{-1} were mainly concentrated in the surface during late summer and autumn, with minima in winter (Molina et al., 2020).
468 However, in our study, heterotrophic bacteria abundance showed no significant differences (p = 0.05) in both periods (1 x 10^6
469 cells/mL) (Fig. S3C and F). This is due to the low DOC at the beginning of the upwelling period (Fig. 2E).

Biogeosciences
Discussions

470   Phase II CH$_4$ accumulation during time incubations under different treatments is shown in Fig. 5. Concentration of cell

471   abundance treatment or concentrated community (CC) resulted in substantial enrichments of cyanobacteria (*Synechoccocus*),

472   picoeukaryotes and heterotrophic bacteria, by factors of 1.9, 1.8 and 4.6, respectively, compared to the NC, and factors of 1.8,

473   1.8 and 6.1 with respect to the <3 µm fraction (Fig. S4A, B and C).In both cases, a substantial increase in bacteria is noted

474   (Fig. S4A, B and C). The microbial abundance proportions in NC at the beginning of the experiment were close to natural

475   observations (Collado-Fabbri et al., 2011; Anabalón et al., 2007; Morales et al., 2007).

476

477

Biogeosciences
Discussions
EGU
Open Access
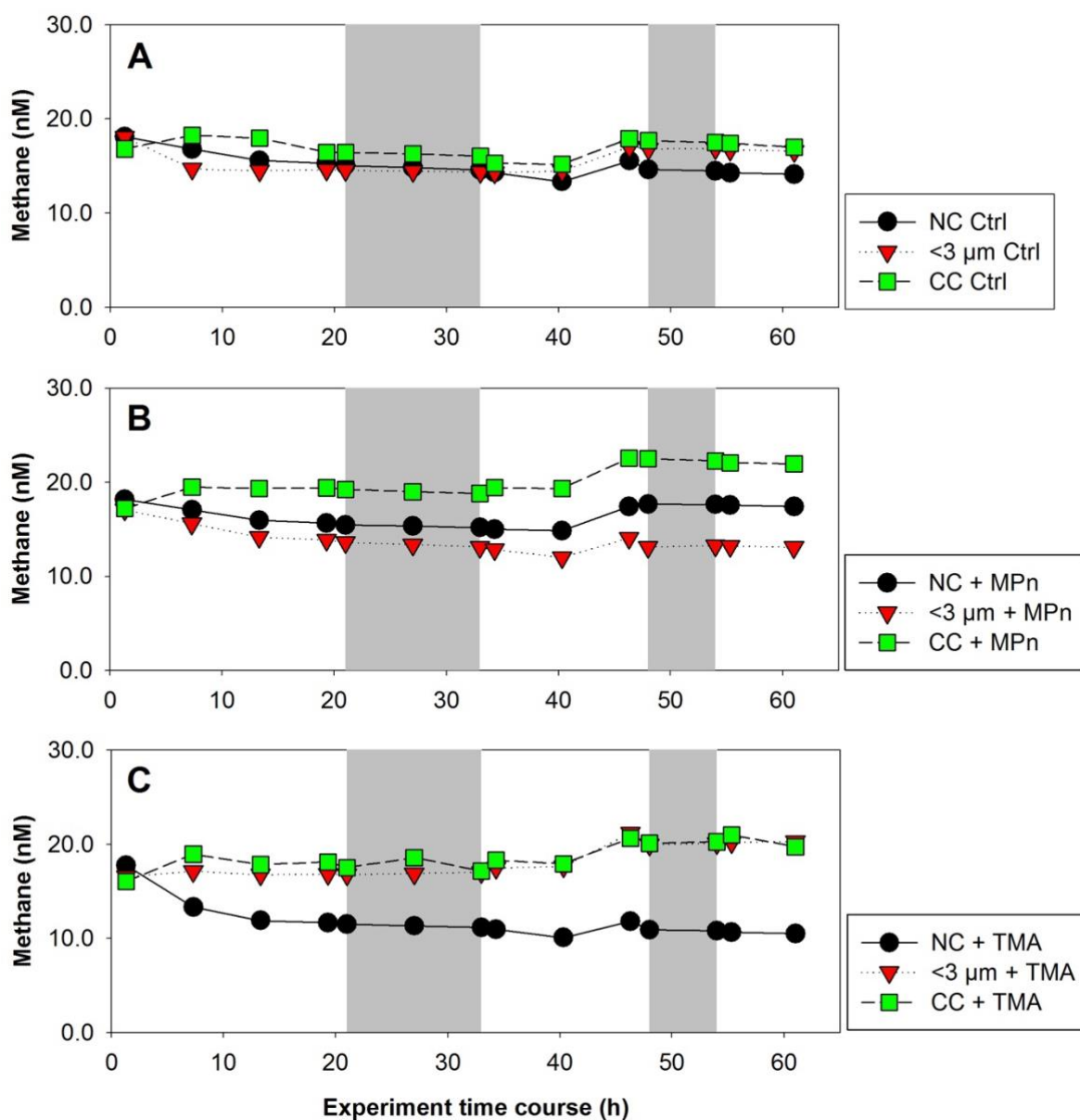
Figure 5. Time courses of dissolved methane (nM) during incubation in long-term microcosm experiments (10L) with the addition of methylated substrates (MPn: methyl phosphonic acid and TMA: trimethylamine) performed with three planktonic communities (NC: natural community; <3 μm: bacterioplankton and CC: community concentrate) under oxygenated conditions in April 2019. Photoperiod is represented in white (light) and gray (dark).

Remarkably, Chl-a levels matched with phytoplankton communities expected in each treatment (Table S3). Mean Chl-a levels in the <3 μm fraction were 21.7 and 4.5 times lower than in the NC and CC, respectively (Table S3), indicating that this fraction contains phyto picoeukaryotes in a lower proportion than CC, and that NC included phyto- microeukaryotes that have the highest Chl-a concentration. Additionally, the CC treatment displayed higher basal levels of DOC and nutrients, due to the natural diurnal mortality of picoplankton (Llabrés et al., 2011) and to the type of filtration, tangential flow filtration, one of the most used methods to concentrate DOM (Benner et al., 1992) that reduces the amount of membrane sorption and fouling and is capable of filtering between 10 to 1000L (Minor et al., 2014).

When comparing the treatments (NC, <3 μm, and CC) without (controls) and with the addition of MPn and TMA (5), significant statistical differences ($p<0.05$) and a similar CH_4 evolution pattern were observed, with a slightly higher CH_4 accumulation during the second photoperiod, especially in the CC and <3 μm fractions (Fig. 5A), indicating that during the first photoperiod there may be changes and/or acclimation of planktonic communities.

With the addition of MPn (Fig. 5B), CH_4 evolution remained constant in the <3 μm fraction, but increased slightly and strongly in the CC and NC, respectively (Fig. 5B). The most significant difference in the CH_4 time course occurred when CC was enriched with MPn (Table S4), suggesting that both heterotrophic bacterioplankton or cyanobacteria could be mediating CH_4 regeneration. Additionally, higher chlorophyll concentrations (Table S3) in NC treatment may have supported greater CH_4 accumulation compared to the <3 μm fraction (Fig. 5B). Regarding TMA enrichment (Fig. 5C), the CC and <3 μm fraction treatments responded similarly, both increasing CH_4 accumulation ($p<0.05$; Fig. 5C). Higher accumulation rates were observed in the <3 μm fraction (Table S4), suggesting that the heterotrophic community present in this period weakly metabolizes TMA (De Angelis and Lee, 1994; Bižić-Ionescu et al., 2018).

Although the conversion of methylated substrates, such as MPn to CH_4 by various types of bacteria has been extensively documented (Repeta et al., 2016; Del Valle and Karl, 2014; Karl et al., 2008; Metcalf et al., 2012; Zhao et al., 2022; Wang et al., 2018; Damm et al., 2010), this process typically occurs under phosphorus-starved conditions. However, it is unlikely in our study area, which experienced high PO_4^{-3} availability and even in excess compared to N (Table 2). Specifically, the expression of phosphonate C-P lyase genes is restrained under P-rich culture conditions (Carini et al., 2014; Taenzer, 2019; Sosa et al., 2019). Thus, an alternative explanation for the significant CH_4 accumulation in the CC with MPn treatment could be related to the presence of cyanobacteria, since using stable isotope labelling techniques recently has shown that CH_4 production comes from cyanobacteria such as *Synechococcus* (Klintzsch et al., 2023). Given that *Synechococcus* dominated during the non-upwelling period (autumn winter season) in the photic layer (Collado-Fabbri et al., 2011) it is plausible to consider CH_4 generation mediated by this microorganism in our upwelling system.

512 Consequently, CH_4 generation pathways appear multifaceted, involving complex interplays between photochemical and

513 metabolic processes. The mechanism by which cyanobacteria effectively convert fixed CO_2 to CH_4 under light conditions

514 appears intricately linked to the photosynthetic process (Bižić et al., 2020; Klintzsch et al., 2020), since inhibitors of

515 photosynthesis blocked CH_4 production under light conditions (Bižić et al., 2020). This suggested that distinct mechanisms

516 might govern CH_4 production under light and dark conditions, influenced by freshly synthesized photosynthetic products in

517 light and storage compounds in darkness.

518 During the high productivity period (Phase I), temporal CH_4 accumulation consistently demonstrated higher CH_4 levels in the

519 CC treatment compared to the NC and <3 μm fraction (controls) (Fig. 6A). However, a noteworthy contrast appears when

520 considering the impact of substrate additions. Specifically, in this phase, the introduction of TMA in the CC treatment results

521 in a more pronounced CH_4 regeneration (Fig. 6C) compared to the effect of MPn (Fig. 6B). This pattern, the opposite of that

522 found in Phase II, could potentially be explained by the observed decrease in *Synechococcus* abundance (Fig. S3D), which

523 remains unresponsive to MPn, and the concurrent increase in nano and picoeucaryotes and bacteria at the end of the experiment

524 (Fig. S3E and F), the last of which is conducive to the action of TMA (Bižić-Ionescu et al., 2018; De Angelis and

525 Lee, 1994; Lidbury et al., 2015). Indeed, a marked reduction in *Synechococcus* abundance was observed (showing a

526 4.6-fold decrease) compared to the transition period (Fig. S4A and D), whereas nano- and picoeukaryotes experienced a notable

527 abundance (3.1 to 3.7 times higher than the transition period) (Fig. S3B and E).

528
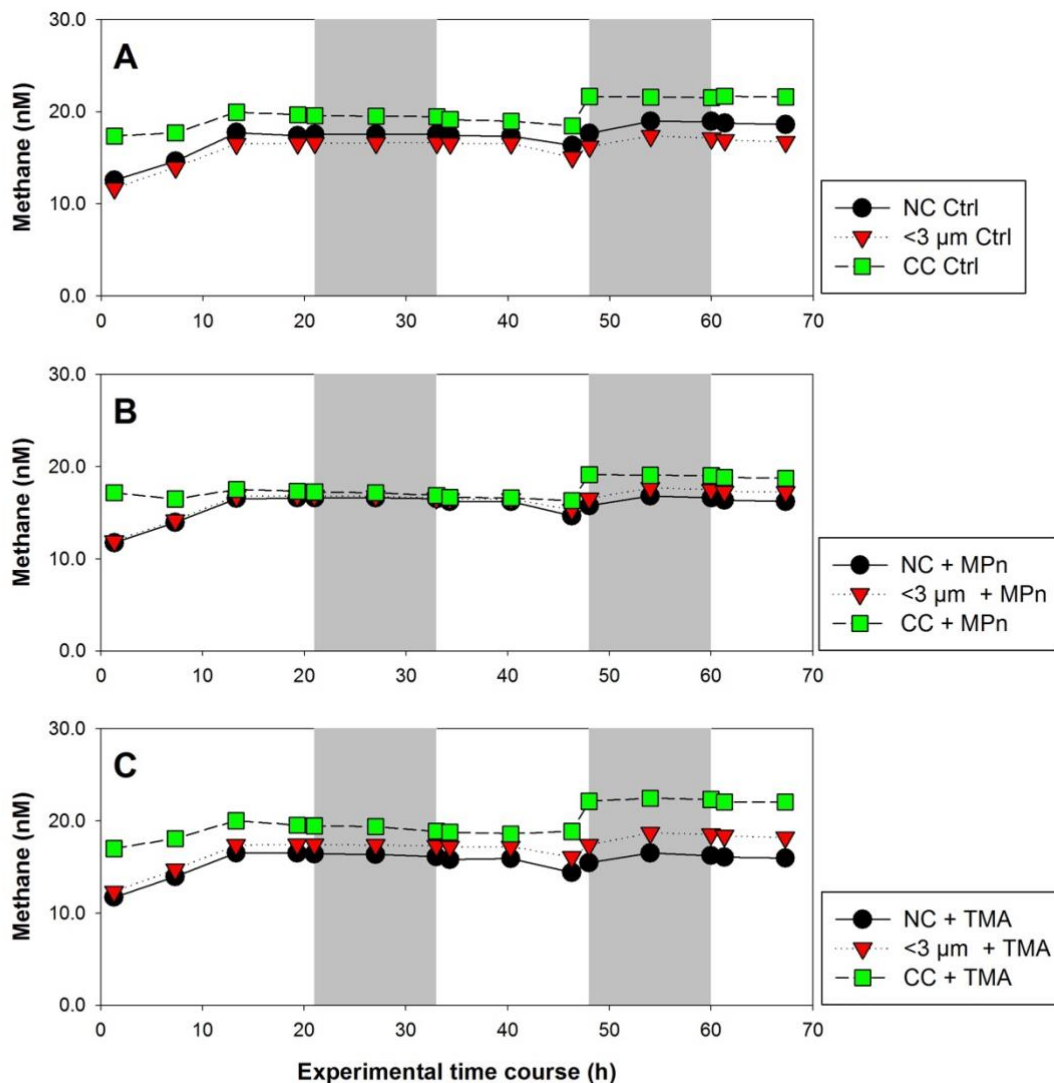
Biogeosciences
Discussions

In this phase, the distribution proportions within the NC treatment were as follows: cyanobacteria, nano and picoeukaryotes, and bacteria accounted for 1.1, 2.3 and 96.6, respectively. In contrast, within the CC treatment, the initial distribution

23

537 proportions were higher with respect to the NC: cyanobacteria, picoeukaryotes, and bacterioplankton displayed proportions
538 1.6, 0.6, and 2.9 times greater, respectively. This underscores the increased significance of bacteria and autotrophic
539 picoeukaryotes during this phase, as further corroborated by Chl-a measurements (Table S3).

540 An intricate interplay between microbial communities and CH_4 cycling within distinct phases of productivity is elucidated
541 (Fig. 7). The prevalence of cyanobacteria, picoeukaryotes, and heterotrophic bacteria varied significantly between these
542 phases. So, this indicates that substrate utilization is related to the availability of nutrients as well as the complexity of the
543 substrate and the composition of the heterotrophic bacterial community, which depends on the productivity phases, potentially
544 driving CH_4 production dynamics.

545
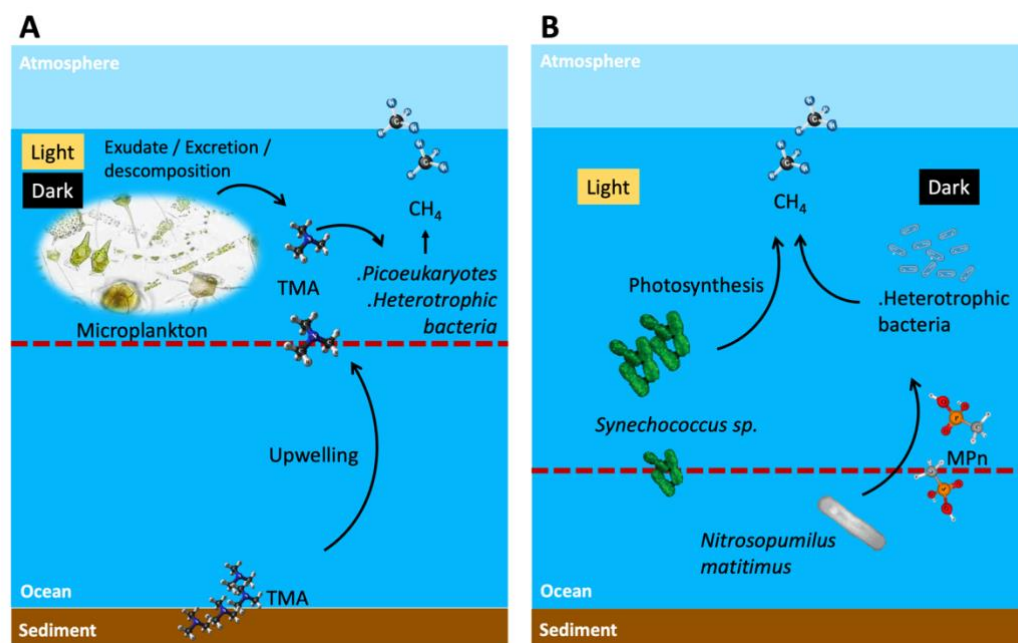
546
547 **Figure 7. Suggested scheme of methane cycling mechanisms in two contrasting periods of primary production and oceanographic**
548 **conditions during light and dark phases, where potential planktonic communities and methylated substrates are involved to**
549 **metabolize methane in surface waters. A. Phase I or active upwelling season and B. Phase II and III or late upwelling or non-**
550 **upwelling season. Dashed line shows the 100 μmol L^{-1} oxycline, above this line oxic methane is produced. TMA: trimethylamine:**
551 **and MPn: methyl phosphonic acid.**

552

553 CC treatment always exhibited elevated CH_4 levels and therefore reflects the relative dominance of cyanobacteria in Phase II
554 (autumn-winter), which are mediating CH_4 cycling via MPn. Indeed, high CH_4 levels in surface water observed in the non-
555 upwelling period, even comparable to upwelling period, could be due to *in situ* production mediated by *Synechoccocus*, or
556 archaea such as *Nitrosopumilus maritimus* that are providing MPn to heterotrophic bacteria to be metabolized (cleaved) and

557   subsequently release CH$_4$ (Fig. 7A). On the other hand, although the trimethylamine methyltransferase enzyme has been

558   described as involved in the demethylation of TMA in methanogen microorganisms (Paul et al., 2000), it cannoted be ruled

559   out that in the upwelling period, heterotrophic bacteria dominance in spring time can metabolize TMA through an alternative

560   pathway still unknown (Fig. 7B). Nor can it be ruled out that the upwelling brings methanogens with the necessary machinery

561   to metabolize TMA at the ocean surface.

562   **4 Conclusions**

563   Overall, picoplankton recycled CH$_4$ in all experiments conducted in both light and dark conditions, although the net CH$_4$

564   production rate was higher in dark conditions. Moreover, laboratory experiments demonstrated that organic compounds such

565   as TMA and MPn are metabolized by heterotrophic bacterioplankton, contributing to the recycling of oxic CH$_4$ in the

566   oxygenated surface layer. This reflects the importance of these microorganisms in the gas' cycling, which could be sustaining

567   the supersaturations and the presence of CH$_4$ hotspots in the surface layer.

568   Coastal upwelling could bring with it organic compounds such as TMA from sediments, which added to plankton

569   decomposition compounds (e.g. TMA), and change in picoplanktonic composition (bacteria and the remarkable increase of

570   pico- and nanoeukaryotes) during the favorable upwelling period, could promote recycling CH$_4$ via TMA, through a pathway

571   that is still unknown, but would potentially add to CH$_4$ supersaturation in the oxygenated surface layer, beyond the contribution

572   of CH$_4$ by advection.

573   *Synechococcus* could be responsible for CH$_4$ regeneration through photosynthesis. These cyanobacteria are abundant in the

574   non-upwelling period, and together with other picoeukaryotes, maintain intermediate and basal Chl-a levels during this period

575   that matched with higher DOC levels and inorganic N:P ratios (compared to the upwelling period). This may stimulate

576   heterotrophic bacteria to metabolize MPn and thus contribute to the recycling of oxic CH$_4$.

577   It important to note that amended experiments were conducted in Phase II (March 2019) and phase III (May 2019), periods

578   marked by changes in the phytoplankton succession (composition), biomass and abundance (Testa et al., 2018). In winter, the

579   relative abundance of picoplankton with respect to microplankton (particularly the presence of *Synechococcus and nitrifying*

580   *archaea)* increases significantly, especially photosynthetic picoeukaryotes (Collado-Fabbri et al., 2011).

588

References

Aguirre, C., Garreaud, R., Belmar, L., Farías, L., Ramajo, L., and Barrera, F.: High-Frequency Variability of the Surface Ocean Properties Off Central Chile During the Upwelling Season, Front Mar Sci, 8, 1–19, https://doi.org/10.3389/fmars.2021.702051, 2021.

Aldunate, M., De la Iglesia, R., Bertagnolli, A. D., and Ulloa, O.: Oxygen modulates bacterial community composition in the coastal upwelling waters off central Chile, Deep Sea Research Part II Topical Studies in Oceanography, 156, 68–79, https://doi.org/10.1016/j.dsr2.2018.02.001, 2018.

Allen, L. Z., Allen, E. E., Badger, J. H., McCrow, J. P., Paulsen, I. T., Elbourne, L. D., Thiagarajan, M., Rusch, D. B., Nealson, K. H., Williamson, S. J., Venter, J. C., and Allen, A. E.: Influence of nutrients and currents on the genomic composition of microbes across an upwelling mosaic, ISME Journal, 6, 1403–1414, https://doi.org/10.1038/ismej.2011.201, 2012.

Anabalón, V., Morales, C. E., Escribano, R., Varas, A. M., and Varas, M. A.: The contribution of nano- and micro-planktonic assemblages in the surface layer (0-30 m) under different hydrographic conditions in the upwelling area off Concepción, central Chile, Prog Oceanogr, 75, 396–414, https://doi.org/10.1016/j.pocean.2007.08.023, 2007.

De Angelis, M. A. and Lee, C.: Methane production during zooplankton grazing on marine phytoplankton, Limnol. Oceanogr., 39, 1298–1308, 1994.

Azam, F. and Malfatti, F.: Microbial structuring of marine ecosystems, Nat Rev Microbiol, 5, 782–791, https://doi.org/10.1038/nrmicro1747, 2007.

Azam, F., Fenchel, T., Field, J., Gray, J., Meyer-Reil, L., and Thingstad, F.: The Ecological Role of Water-Column Microbes in the Sea, Mar Ecol Prog Ser, 10, 257–263, https://doi.org/10.3354/meps010257, 1983.

Bange, H. W., Bartell, U. H., Rapsomanikis, S., and Andreae, M. O.: Methane in the Baltic and North Seas and a reassessment of the marine emissions of methane, Global Biogeochem Cycles, 8, 465–480, 1994.

Bates, T. S., Kelly, K. C., Johnson, J. E., and Gammon, R. H.: A reevaluation of the open ocean source of methane to the atmosphere, Journal of Geophysical Research Atmospheres, 101, 6953–6961, https://doi.org/10.1029/95JD03348, 1996.

Bauer, J. and Druffel, E.: Ocean margins as a significant source of organic matter to the deep open ocean, Letter to nature, 392, 482–485, https://doi.org/https://doi.org/10.1038/33122, 1998.

Bello, E.: Variabilidad estacional en la descarga de metano disuelto desde un sistema estuarino a la zona marina adyacente, el caso de ríos de la zona central de chile (río Itata), Universidad de Concepción, 76 pp., 2016.

Belviso, S., Kim, S. -K, Rassoulzadegan, F., Krajka, B., Nguyen, B. C., Mihalopoulos, N., and Buat-Menard, P.: Production of dimethylsulfonium propionate (DMSP) and dimethylsulfide (DMS) by a microbial food web, Limnol Oceanogr, 35, 1810–1821, https://doi.org/10.4319/lo.1990.35.8.1810, 1990.

Benner, R., Dean Pakulski, J., Mccarthy, M., Hedges, J. I., Hatcher, P. G., Benner, R., Pakulski, J. D., McCarthy, M., Hedges, J. I., Hatcher, P. G., H van Beest, B. W., Kramer, G. J., and van Santen, R. A.: Bulk chemical characteristics of dissolved organic matter in the ocean, J. Glinnemann, ibid, 255, 1561–1564, https://doi.org/DOI: 10.1126/science.255.5051.1561, 1992.

622 Berg, A., Lindblad, P., and Svensson, B. H.: Cyanobacteria as a source of hydrogen for methane formation, World J Microbiol
623 Biotechnol, 30, 539–545, https://doi.org/10.1007/s11274-013-1463-5, 2014.

624 Bizic, M.: Phytoplankton photosynthesis: An unexplored source of biogenic methane emission from oxic environments, J
625 Plankton Res, 43, 822–830, https://doi.org/10.1093/plankt/fbab069, 2021.

626 Bižić, M., Klintzsch, T., Ionescu, D., Hindiyeh, M. Y., Günthel, M., Muro-Pastor, A. M., Eckert, W., Urich, T., Keppler, F.,
627 and Grossart, H. P.: Aquatic and terrestrial cyanobacteria produce methane, Sci Adv, 6, 1–10,
628 https://doi.org/10.1126/sciadv.aax5343, 2020.

629 Bižić-Ionescu, M., Ionescu, D., Günthel, M., Tang, K. W., and Grossart, H. P.: Oxic Methane Cycling: New Evidence for
630 Methane Formation in Oxic LakeWater, Biogenesis of Hydrocarbons, 1–22, https://doi.org/10.1007/978-3-319-53114-4, 2018.

631 Brown, I. J., Torres, R., and Rees, A. P.: The origin of sub-surface source waters define the sea-air flux of methane in the
632 Mauritanian Upwelling, NW Africa, Dynamics of Atmospheres and Oceans, 67, 39–46,
633 https://doi.org/10.1016/j.dynatmoce.2014.06.001, 2014.

634 Bullister, J. L., Wisegarver, D. P., and Wilson, S. T.: The production of Methane and Nitrous Oxide Gas Standards for
635 Scientific Committee on Ocean Research (SCOR) Working Group #143, 1–9 pp., 2016.

636 Capelle, D. W. and Tortell, P. D.: Factors controlling methane and nitrous-oxide variability in the southern British Columbia
637 coastal upwelling system, Mar Chem, 179, 56–67, https://doi.org/10.1016/j.marchem.2016.01.011, 2016.

638 Carini, P., White, A. E., Campbell, E. O., and Giovannoni, S. J.: Methane production by phosphate-starved SAR11
639 chemoheterotrophic marine bacteria, Nat Commun, 5, 1–7, https://doi.org/10.1038/ncomms5346, 2014.

640 Carpenter, L. J., Archer, S. D., and Beale, R.: Ocean-atmosphere trace gas exchange, Chem Soc Rev, 41, 6473–6506,
641 https://doi.org/10.1039/c2cs35121h, 2012.

642 Cerbin, S., Pérez, G., Rybak, M., Wejnerowski, Ł., Konowalczyk, A., Helmsing, N., Naus-Wiezer, S., Meima-Franke, M.,
643 Pytlak, Ł., Raaijmakers, C., Nowak, W., and Bodelier, P. L. E.: Methane-Derived Carbon as a Driver for Cyanobacterial
644 Growth, Front Microbiol, 13, 1–16, https://doi.org/10.3389/fmicb.2022.837198, 2022.

645 Codispoti, L. A.: Is the ocean losing nitrate?, Nature, 376, 724, https://doi.org/https://doi.org/10.1038/376724a0, 1995.

646 Collado-Fabbri, S., Vaulot, D., and Ulloa, O.: Structure and seasonal dynamics of the eukaryotic picophytoplankton
647 community in a wind-driven coastal upwelling ecosystem, Limnol. Oceanogr., 56, 2334–2346,
648 https://doi.org/10.4319/lo.2011.56.6.2334, 2011.

649 Cuevas, L. A., Daneri, G., Jacob, B., and Montero, P.: Microbial abundance and activity in the seasonal upwelling area off
650 Concepción (~36°S), central Chile: A comparison of upwelling and non-upwelling conditions, Deep Sea Res 2 Top Stud
651 Oceanogr, 51, 2427–2440, https://doi.org/10.1016/j.dsr2.2004.07.026, 2004.

652 Damm, E., Helmke, E., Thoms, S., Schauer, U., Nöthig, E., Bakker, K., and Kiene, R. P.: Methane production in aerobic
653 oligotrophic surface water in the central Arctic Ocean, Biogeosciences, 7, 1099–1108, https://doi.org/10.5194/bgd-6-10355-
654 2009, 2010.

Biogeosciences
Discussions
Open Access
EGU

655   Dinasquet, J., Tiirola, M., and Azam, F.: Enrichment of Bacterioplankton Able to Utilize One-Carbon and Methylated
656   Compounds in the Coastal Pacific Ocean, Front Mar Sci, 5, 1–13, https://doi.org/10.3389/fmars.2018.00307, 2018.

657   Donis, D., Flury, S., Stöckli, A., Spangenberg, J. E., Vachon, D., and McGinnis, D. F.: Full-scale evaluation of methane
658   production under oxic conditions in a mesotrophic lake, Nat Commun, 8, 1–11, https://doi.org/10.1038/s41467-017-01648-4,
659   2017.

660   Dumestre, J. F., Guézennec, J., Galy-Lacaux, C., Delmas, R., Richard, S., and Labroue, L.: Influence of light intensity on
661   methanotrophic bacterial activity in Petit Saut Reservoir, French Guiana, Appl Environ Microbiol, 65, 534–539,
662   https://doi.org/10.1128/aem.65.2.534-539.1999, 1999.

663   Emeis, K., Eggert, A., Flohr, A., Lahajnar, N., Nausch, G., Neumann, A., Rixen, T., Schmidt, M., Van der Plas, A., and
664   Wasmund, N.: Biogeochemical processes and turnover rates in the Northern Benguela Upwelling System, Journal of Marine
665   Systems, 188, 63–80, https://doi.org/10.1016/j.jmarsys.2017.10.001, 2018.

666   Farías, L., Graco, M., and Ulloa, O.: Temporal variability of nitrogen cycling in continental-shelf sediments of the upwelling
667   ecosystem off central Chile, Deep Sea Res 2 Top Stud Oceanogr, 51, 2491–2505, https://doi.org/10.1016/j.dsr2.2004.07.029,
668   2004.

669   Farías, L., Fernández, C., Faúndez, J., Cornejo, M., and Alcaman, M. E.: Chemolithoautotrophic production mediating the
670   cycling of the greenhouse gases N2O and CH4 in an upwelling ecosystem, Biogeosciences, 6, 3053–3069,
671   https://doi.org/https://doi.org/10.5194/bg-6-3053-2009, 2009.

672   Farías, L., Besoain, V., and García-Loyola, S.: Presence of nitrous oxide hotspots in the coastal upwelling area off central
673   Chile: An analysis of temporal variability based on ten years of a biogeochemical time series, Environmental Research Letters,
674   10, 1–13, https://doi.org/10.1088/1748-9326/10/4/044017, 2015.

675   Farías, L., Tenorio, S., Sanzana, K., and Faundez, J.: Temporal methane variability in the water column of an area of seasonal
676   coastal upwelling: A study based on a 12 year time series, Prog Oceanogr, 195, https://doi.org/10.1016/j.pocean.2021.102589,
677   2021.

678   Fazi, S., Amalfitano, S., Venturi, S., Pacini, N., Vazquez, E., Olaka, L. A., Tassi, F., Crognale, S., Herzsprung, P., Lechtenfeld,
679   O. J., Cabassi, J., Capecchiacci, F., Rossetti, S., Yakimov, M. M., Vaselli, O., Harper, D. M., and Butturini, A.: High
680   concentrations of dissolved biogenic methane associated with cyanobacterial blooms in East African lake surface water,
681   Commun Biol, 4, 1–12, https://doi.org/10.1038/s42003-021-02365-x, 2021.

682   Ferderlman, T. G., Lee, C., Pantoja, S., Harder, J., Bebout, B. M., and Fossing, H.: Sulfate reduction and methanogenesis in a
683   Thioploca- dominates sediment off the coast of Chile, Geochim Cosmochim Acta, 61, 3065–3079,
684   https://doi.org/https://doi.org/10.1016/S0016-7037(97)00158-0, 1997.

685   Fernandez, C. and Farías, L.: Assimilation and regeneration of inorganic nitrogen in a coastal upwelling system: Ammonium
686   and nitrate utilization, Mar Ecol Prog Ser, 451, 1–14, https://doi.org/10.3354/meps09683, 2012.

687   Fernandez, C., González, M. L., Muñoz, C., Molina, V., and Farias, L.: Temporal and spatial variability of biological nitrogen
688   fixation off the upwelling system of central Chile (35-38.5°S), J Geophys Res Oceans, 120, 3330–3349,
689   https://doi.org/10.1002/2014JC010410, 2015.

690   Florez-Leiva, L., Damm, E., Farías, L., and Farias, L.: Methane production induced by dimethylsulfide in surface water of an
691   upwelling ecosystem, Prog Oceanogr, 112–113, 38–48, https://doi.org/10.1016/j.pocean.2013.03.005, 2013.

692   Gibb, S. W., Mantoura, R. F. C., Liss, P. S., and Barlow, R. G.: Distributions and biogeochemistries of methylamines and
693   ammonium in the Arabian Sea, Deep Sea Res 2 Top Stud Oceanogr, 46, 593–615, https://doi.org/10.1016/S0967-
694   0645(98)00119-2, 1999.

695   Giovannoni, S. J., Delong, E. F., Schmidt, T. M., and Pace, N. R.: Tangential Flow Filtration and Preliminary Phylogenetic
696   Analysis of Marine Picoplankton, Appl Environ Microbiol, 56, 2572–2575, 1990.

697   González, H. E., Menschel, E., Aparicio, C., and Barría, C.: Spatial and temporal variability of microplankton and detritus,
698   and their export to the shelf sediments in the upwelling area off Concepción, Chile (~36°S), during 2002-2005, Prog Oceanogr,
699   75, 435–451, https://doi.org/10.1016/j.pocean.2007.08.025, 2007.

700   Grossart, H. P., Frindte, K., Dziallas, C., Eckert, W., and Tang, K. W.: Microbial methane production in oxygenated water
701   column of an oligotrophic lake, Proc Natl Acad Sci U S A, 108, 19657–19661, https://doi.org/10.1073/pnas.1110716108,
702   2011.

703   Günthel, M., Donis, D., Kirillin, G., Ionescu, D., Bizic, M., McGinnis, D. F., Grossart, H. P., and Tang, K. W.: Contribution
704   of oxic methane production to surface methane emission in lakes and its global importance, Nat Commun, 10,
705   https://doi.org/10.1038/s41467-019-13320-0, 2019.

706   Günthel, M., Klawonn, I., Woodhouse, J., Bižić, M., Ionescu, D., Ganzert, L., Kümmel, S., Nijenhuis, I., Zoccarato, L.,
707   Grossart, H. P., and Tang, K. W.: Photosynthesis-driven methane production in oxic lake water as an important contributor to
708   methane emission, Limnol Oceanogr, 1–13, https://doi.org/10.1002/lno.11557, 2020.

709   Hahn, M. W.: Broad diversity of viable bacteria in "sterile" (0.2 μm) filtered water, Res Microbiol, 155, 688–691,
710   https://doi.org/10.1016/j.resmic.2004.05.003, 2004.

711   Hansell, D. A. and Orellana, M. V.: Dissolved organic matter in the global ocean: A primer, Gels, 7, 1–8,
712   https://doi.org/10.3390/gels7030128, 2021.

713   Harmsen, M., van Vuuren, D. P., Bodirsky, B. L., Chateau, J., Durand-Lasserve, O., Drouet, L., Fricko, O., Fujimori, S.,
714   Gernaat, D. E. H. J., Hanaoka, T., Hilaire, J., Keramidas, K., Luderer, G., Moura, M. C. P., Sano, F., Smith, S. J., and Wada,
715   K.: The role of methane in future climate strategies: mitigation potentials and climate impacts, Clim Change, 163, 1409–1425,
716   https://doi.org/10.1007/s10584-019-02437-2, 2020.

717   Hartmann, J. F., Günthel, M., Klintzsch, T., Kirillin, G., Grossart, H. P., Keppler, F., and Isenbeck-Schröter, M.: High
718   Spatiotemporal Dynamics of Methane Production and Emission in Oxic Surface Water, Environ Sci Technol, 54, 1451–1463,
719   https://doi.org/10.1021/acs.est.9b03182, 2020.

720 Herndl, G. and Malacic, V.: Impact of the pycnocline layer on bacterioplankton: diel and spatial variations in microbial
721 parameters in the stratified water column of the Gulf of Trieste (Northern Adriatic Sea), Mar Ecol Prog Ser, 38, 295–303,
722 https://doi.org/10.3354/meps038295, 1987.

723 Holmkvist, L., Arning, E. T., Küster-Heins, K., Vandieken, V., Peckmann, J., Zabel, M., and Jørgensen, B. B.: Phosphate
724 geochemistry, mineralization processes, and Thioploca distribution in shelf sediments off central Chile, Mar Geol, 277, 61–
725 72, https://doi.org/10.1016/j.margeo.2010.08.011, 2010.

726 Igarza, M., Dittmar, T., Graco, M., and Niggemann, J.: Dissolved organic matter cycling in the coastal upwelling system off
727 central Peru during an "El Niño" year, Front Mar Sci, 6, 1–17, https://doi.org/10.3389/fmars.2019.00198, 2019.

728 IPCC: Climate Change 2021: The Physical Science Basis. Working Group I Contribution to the IPCC Sixth Assessment
729 Report, Cambridge University Press, 35–144 pp., 2021.

730 Johnson, P. W. and Sieburth, J. M. N.: Chroococcoid cyanobacteria in the sea: A ubiquitous and diverse phototrophic biomass,
731 Limnol Oceanogr, 24, 928–935, https://doi.org/10.4319/lo.1979.24.5.0928, 1979.

732 Kara, A. B., Rochford, P. A., and Hurlburt, H. E.: Mixed layer depth variability over the global ocean, J Geophys Res Oceans,
733 108, 1–15, https://doi.org/10.1029/2000jc000736, 2003.

734 Karl, D., Beversdorf, L., Björkman, K., Church, M., Martinez, A., and DeLong, E.: Aerobic production of methane in the sea,
735 Nat Geosci, 1, 473–478, https://doi.org/10.1038/ngeo234, 2008.

736 Kelley, C. A. and Jeffrey, W. H.: Dissolved methane concentration profiles and air-sea fluxes from 41°S to 27°N, Global
737 Biogeochem Cycles, 16, 1–6, https://doi.org/10.1029/2001gb001809, 2002.

738 Klintzsch, T., Langer, G., Nehrke, G., Wieland, A., Lenhart, K., and Keppler, F.: Methane production by three widespread
739 marine phytoplankton species: release rates, precursor compounds, and relevance for the environment, Biogeosciences, 16,
740 4129–4144, https://doi.org/10.5194/bg-2019-245, 2019.

741 Klintzsch, T., Langer, G., Wieland, A., Geisinger, H., Lenhart, K., Nehrke, G., and Keppler, F.: Effects of Temperature and
742 Light on Methane Production of Widespread Marine Phytoplankton, J Geophys Res Biogeosci, 125, 1–16,
743 https://doi.org/10.1029/2020JG005793, 2020.

744 Klintzsch, T., Geisinger, H., Wieland, A., Langer, G., Nehrke, G., Bizic, M., Greule, M., Lenhart, K., Borsch, C., Schroll, M.,
745 and Keppler, F.: Stable Carbon Isotope Signature of Methane Released From Phytoplankton, Geophys Res Lett, 50, 1–12,
746 https://doi.org/10.1029/2023gl103317, 2023.

747 Kock, A., Gebhardt, S., and Bange, H. W. W.: Methane emissions from the upwelling area off Mauritania (NW Africa),
748 Biogeosciences, 5, 1119–1125, https://doi.org/10.5194/bg-5-1119-2008, 2008.

749 De La Iglesia, R., Echenique-Subiabre, I., Rodríguez-Marconi, S., Espinoza, J. P., Von Dassow, P., Ulloa, O., and Trefault,
750 N.: Distinct oxygen environments shape picoeukaryote assemblages thriving oxygen minimum zone waters off central Chile,
751 J Plankton Res, 42, 514–529, https://doi.org/10.1093/plankt/fbaa036, 2020.

752 Lamontagne, R. A., Swinnerton, J. W., Linnenbom, V. J., and Smith, W. D.: Methane Concentrations in Various Marine
753 Environments, J Geophys Res, 78, 5317–5324, https://doi.org/10.1029/JC078i024p05317, 1973.

754   Lenhart, K., Klintzsch, T., Langer, G., Nehrke, G., Bunge, M., Schnell, S., and Keppler, F.: Evidence for methane production

755   by the marine algae Emiliania huxleyi, Biogeosciences, 13, 3163–3174, https://doi.org/10.5194/bg-13-3163-2016, 2016.

756   León-Palmero, E., Contreras-Ruiz, A., Sierra, A., Morales-Baquero, R., and Reche, I.: Dissolved CH_4 coupled to

757   photosynthetic picoeukaryotes in oxic waters and to cumulative chlorophyll a in anoxic waters of reservoirs, Biogeosciences,

758   17, 1–23, https://doi.org/10.5194/bg-17-3223-2020, 2020.

759   Li, Y., Fichot, C. G., Geng, L., Scarratt, M. G., and Xie, H.: The Contribution of Methane Photoproduction to the Oceanic

760   Methane Paradox, Geophys Res Lett, 47, 1–10, https://doi.org/10.1029/2020GL088362, 2020.

761   Lidbury, I. D. E. A., Murrell, J. C., and Chen, Y.: Trimethylamine and trimethylamine N-oxide are supplementary energy

762   sources for a marine heterotrophic bacterium: Implications for marine carbon and nitrogen cycling, ISME Journal, 9, 760–769,

763   https://doi.org/10.1038/ismej.2014.149, 2015.

764   Liu, L.-Y., Xie, G.-J., Ding, J., Liu, B.-F., Xing, D.-F., Ren, N.-Q., and Wang, Q.: Microbial methane emissions from the non-

765   methanogenesis processes: A critical review, Science of the Total Environment, 806, 1–11,

766   https://doi.org/10.1016/j.scitotenv.2021.151362, 2022.

767   Llabrés, M., Agustí, S., and Herndl, G. J.: Diel in situ picophytoplankton cell death cycles coupled with cell division, J Phycol,

768   47, 1247–1257, https://doi.org/10.1111/j.1529-8817.2011.01072.x, 2011.

769   Lohrer, C., Cwierz, P. P., Wirth, M. A., Schulz-Bull, D. E., and Kanwischer, M.: Methodological aspects of methylphosphonic

770   acid analysis: Determination in river and coastal water samples, Talanta, 211, 1–8,

771   https://doi.org/10.1016/j.talanta.2020.120724, 2020.

772   Macías-Zamora, J.: Dissolved methane in the sills region of the Gulf of California, Cienc Mar, 39, 119–135,

773   https://doi.org/10.7773/cm.v39i2.2232, 2013.

774   McAuliffe, C.: Solubility in water of C1-C9 hydrocarbons, Nature, 200, 1092–1093, 1963.

775   Metcalf, W. W., Griffin, B. M., Cicchillo, R., Gao, J., Janga, S., Cooke, H., Circello, B., Evans, B., Martens-Habbena, W.,

776   Stahl, D., and Van Der Donk, W.: Synthesis of Methylphosphonic Acid by Marine Microbes: A Source for Methane in the

777   Aerobic Ocean, Science (1979), 337, 1104–1107, https://doi.org/10.1126/science.1219875, 2012.

778   Minor, E. C., Swenson, M. M., Mattson, B. M., and Oyler, A. R.: Structural characterization of dissolved organic matter: A

779   review of current techniques for isolation and analysis, Environmental Sciences: Processes and Impacts, 16, 2064–2079,

780   https://doi.org/10.1039/c4em00062e, 2014.

781   Molina, V., Belmar, L., Levipan, H. A., Ramírez-Flandes, S., Anguita, C., Galán, A., Montes, I., and Ulloa, O.: Spatiotemporal

782   Distribution of Key Pelagic Microbes in a Seasonal Oxygen-Deficient Coastal Upwelling System of the Eastern South Pacific

783   Ocean, Front Mar Sci, 7, 1–17, https://doi.org/10.3389/fmars.2020.561597, 2020.

784   Monteiro, P. M. S., Van Der Plas, A., Mohrholz, V., Mabille, E., Pascall, A., and Joubert, W.: Variability of natural hypoxia

785   and methane in a coastal upwelling system: Oceanic physics or shelf biology?, Geophys Res Lett, 33, 1–5,

786   https://doi.org/10.1029/2006GL026234, 2006.

787 Mopper, K., Kieber, D. J., and Stubbins, A.: Marine Photochemistry of Organic Matter: Processes and Impacts. Processes and
788 Impacts., in: Biogeochemistry of Marine Dissolved Organic Matter: Second Edition, Elsevier Inc., 389–450,
789 https://doi.org/10.1016/B978-0-12-405940-5.00008-X, 2015.

790 Morales, C. and Anabalón, V.: Phytoplankton biomass and microbial abundances during the spring upwelling season in the
791 coastal area off Concepción , central-southern Chile : Variability around a time series station, Prog Oceanogr, 92–95, 81–91,
792 https://doi.org/10.1016/j.pocean.2011.07.004, 2012.

793 Morales, C., González, H. E., Hormazabal, S. E., Yuras, G., Letelier, J., and Castro, L. R.: The distribution of chlorophyll- a
794 and dominant planktonic components in the coastal transition zone off Concepción, central Chile, during different
795 oceanographic conditions, Prog Oceanogr, 75, 452–469, https://doi.org/10.1016/j.pocean.2007.08.026, 2007.

796 Morán, X. A. G., Estrada, M., Gasol, J. M., and Pedrós-Alió, C.: Dissolved primary production and the strength of
797 phytoplankton-bacterioplankton coupling in contrasting marine regions, Microb Ecol, 44, 217–223,
798 https://doi.org/10.1007/s00248-002-1026-z, 2002.

799 Morgan, E. J., Lavric, J. V., Arévalo-Martínez, D. L., Bange, H. W., Steinhoff, T., Seifert, T., and Heimann, M.: Air-sea fluxes
800 of greenhouse gases and oxygen in the northern Benguela Current region during upwelling events, Biogeosciences, 16, 4065–
801 4084, https://doi.org/10.5194/bg-16-4065-2019, 2019.

802 Muñoz-Marín, M. C., Gómez-Baena, G., López-Lozano, A., Moreno-Cabezuelo, J. A., Díez, J., and García-Fernández, J. M.:
803 Mixotrophy in marine picocyanobacteria: use of organic compounds by Prochlorococcus and Synechococcus,
804 https://doi.org/10.1038/s41396-020-0603-9, 1 May 2020.

805 Paul, L., Ferguson, D. J., and Krzycki, J. A.: The Trimethylamine Methyltransferase Gene and Multiple Dimethylamine
806 Methyltransferase Genes of Methanosarcina barkeri Contain In-Frame and Read-Through Amber Codons †, J Bacteriol, 182,
807 2520–2529, https://doi.org/0021-9193/00/$04.00≤0, 2000.

808 Pomeroy, L. R., Williams, P. J. L., Azam, F., and Hobbie, J. E.: The Microbial Loop, Source: Oceanography, 20, 28–33,
809 https://doi.org/https://doi.org/10.5670/oceanog.2007.45, 2007.

810 Rain-Franco, A., Sobarzo, M., Caparros, J., and Fernandez, C.: Variability of chromophoric dissolved organic matter in three
811 freshwater-influenced systems along central-southern Chile, Prog Oceanogr, 174, 154–161,
812 https://doi.org/10.1016/j.pocean.2018.09.009, 2019.

813 Raven, J. A.: The twelfth Tansley Lecture. Small is beautiful: The picophytoplankton, Funct Ecol, 12, 503–513,
814 https://doi.org/10.1046/j.1365-2435.1998.00233.x, 1998.

815 Redfield, A. C., Ketchum, B. H., and Richards, F. A.: The influence of organisms on the composition of sea water, The sea,
816 2, 26–77, 1963.

817 Reeburgh, W. S.: Oceanic methane biogeochemistry, American Chemical Society, 107, 486–513,
818 https://doi.org/10.1021/cr050362v, 2007.

819 Reintjes, G., Fuchs, B. M., Scharfe, M., Wiltshire, K. H., Amann, R., and Arnosti, C.: Short-term changes in polysaccharide
820 utilization mechanisms of marine bacterioplankton during a spring phytoplankton bloom, Environ Microbiol, 22, 1884–1900,
821 https://doi.org/10.1111/1462-2920.14971, 2020.

822 Repeta, D. J., Ferrón, S., Sosa, O. A., Johnson, C. G., Repeta, L. D., Acker, M., DeLong, E. F., and Karl, D. M.: Marine
823 methane paradox explained by bacterial degradation of dissolved organic matter, Nat Geosci, 9, 1–7,
824 https://doi.org/10.1038/ngeo2837, 2016.

825 Sansone, F. J., Popp, B. N., Gasc, A., Graham, A. W., and Rust, T. M.: Highly elevated methane in the Eastern tropical North
826 Pacific and associated isotopically enriched fluxes to the atmosphere, Geophys Res Lett, 28, 4567–4570,
827 https://doi.org/10.1029/2001GL013460, 2001.

828 Saunois, M., Stavert, A. R., Poulter, B., Bousquet, P., Canadell, J. G., Jackson, R. B., Raymond, P. A., Dlugokencky, E. J.,
829 and Houweling, S.: The Global Methane Budget 2000 – 2017, Earth Syst Sci Data, 12, 1561–1623,
830 https://doi.org/10.5194/essd-12-1561-2020, 2020.

831 Sieburth, J., Smetacek, V., and Lenz, J.: Pelagic ecosystem structure: Heterotrophic compartments of the plankton and their
832 relationship to plankton size fractions, Linmol. Oceanogr., 23, 1256–1263, https://doi.org/10.4319/lo.1978.23.6.1256, 1978.

833 Silva, N., Rojas, N., and Fedele, A.: Water masses in the Humboldt Current System: Properties, distribution, and the nitrate
834 deficit as a chemical water mass tracer for Equatorial Subsurface Water off Chile, Deep Sea Research Part II: Topical Studies
835 in Oceanography, 56, 1004–1020, https://doi.org/10.1016/j.dsr2.2008.12.013, 2009.

836 Smith, M. W., Allen, L. Z., Allen, A. E., Herfort, L., and Simon, H. M.: Contrasting genomic properties of free-living and
837 particle-attached microbial assemblages within a coastal ecosystem, Front Microbiol, 4, 1–20,
838 https://doi.org/10.3389/fmicb.2013.00120, 2013.

839 Sobarzo, M. and Djurfeldt, L.: Coastal upwelling process on a continental shelf limited by submarine canyons, Concepción,
840 central Chile, J Geophys Res, 109, 1–20, https://doi.org/10.1029/2004JC002350, 2004.

841 Sobarzo, M., Bravo, L., Donoso, D., Garcés-Vargas, J., and Schneider, W.: Coastal upwelling and seasonal cycles that
842 influence the water column over the continental shelf off central Chile, Prog Oceanogr, 75, 363–382,
843 https://doi.org/10.1016/j.pocean.2007.08.022, 2007.

844 Sosa, O. A., Repeta, D. J., DeLong, E. F., Ashkezari, M. D., and Karl, D. M.: Phosphate-limited ocean regions select for
845 bacterial populations enriched in the carbon–phosphorus lyase pathway for phosphonate degradation, Environ Microbiol, 21,
846 2402–2414, https://doi.org/10.1111/1462-2920.14628, 2019.

847 Sosa, O. A., Burrell, T. J., Wilson, S. T., Foreman, R. K., Karl, D. M., and Repeta, D. J.: Phosphonate cycling supports methane
848 and ethylene supersaturation in the phosphate-depleted western North Atlantic Ocean, Limnol Oceanogr, 1–17,
849 https://doi.org/10.1002/lno.11463, 2020.

850 Spilling, K., Camarena-Gómez, M. T., Lipsewers, T., Martinez-Varela, A., Díaz-Rosas, F., Eronen-Rasimus, E., Silva, N., von
851 Dassow, P., and Montecino, V.: Impacts of reduced inorganic N:P ratio on three distinct plankton communities in the Humboldt
852 upwelling system, Mar Biol, 166, 1–17, https://doi.org/10.1007/s00227-019-3561-x, 2019.

853 Stefels, J. and Van Boekel, W.: Production of DMS from dissolved DMSP in axenic cultures of the marine phytoplankton
854 species Phaeocystis sp, Mar Ecol Prog Ser, 97, 11–18, https://doi.org/https://www.jstor.org/stable/24833593, 1993.

855 Strub, T., Mesías, J., Montecino, V., Rutllant, J., and Salinas, S.: Coastal ocean circulation off western south america, in: The
856 global coastal ocean - regional studies and syntheses, vol. 11, 273–313, 1998.

857 Sun, J., Steindler, L., Thrash, J. C., Halsey, K. H., Smith, D. P., Carter, A. E., Landry, Z. C., and Giovannoni, S. J.: One Carbon
858 Metabolism in SAR11 Pelagic Marine Bacteria, PLoS One, 6, 1–12, https://doi.org/10.1371/journal.pone.0023973, 2011.

859 Sun, J., Mausz, M. A., Chen, Y., and Giovannoni, S. J.: Microbial trimethylamine metabolism in marine environments, Environ
860 Microbiol, 21, 513–520, https://doi.org/10.1111/1462-2920.14461, 2019.

861 Taenzer, L.: The isotope biogeochemistry of methane produced from the C-P lyase pathway, Dartmouth College, 2019.

862 Tang, K. W., McGinnis, D. F., Ionescu, D., and Grossart, H. P.: Methane production in oxic lake waters potentially increases
863 aquatic methane flux to air, Environ Sci Technol Lett, 3, 227–233, https://doi.org/10.1021/acs.estlett.6b00150, 2016.

864 Testa, G., Masotti, I., and Farías, L.: Temporal Variability in Net Primary Production in an Upwelling Area off Central Chile
865 (36°S), Front Mar Sci, 5, 1–17, https://doi.org/10.3389/fmars.2018.00179, 2018.

866 Thornton, D. C. O.: Dissolved organic matter (DOM) release by phytoplankton in the contemporary and future ocean, Eur J
867 Phycol, 49, 20–46, https://doi.org/10.1080/09670262.2013.875596, 2014.

868 Del Valle, D. A. and Karl, D. M.: Aerobic production of methane from dissolved water-column methylphosphonate and sinking
869 particles in the North Pacific Subtropical Gyre, Aquatic Microbial Ecology, 73, 93–105, https://doi.org/10.3354/ame01714,
870 2014.

871 Vargas, C. A., Arriagada, L., Sobarzo, M., Contreras, P. Y., and Saldías, G.: Bacterial production along a river-to-ocean
872 continuum in central Chile: Implications for organic matter cycling, Aquatic Microbial Ecology, 68, 195–213,
873 https://doi.org/10.3354/ame01608, 2013.

874 Vargas, C. A., Contreras, P. Y., Pérez, C. A., Sobarzo, M., Saldías, G. S., and Salisbury, J.: Influences of riverine and upwelling
875 waters on the coastal carbonate system off Central Chile and their ocean acidification implications, J Geophys Res Biogeosci,
876 121, 1–16, https://doi.org/10.1002/2015JG003213, 2016.

877 Wang, Q., Dore, J. E., and McDermott, T. R.: Methylphosphonate Metabolism by Pseudomonas sp . Populations Contributes
878 to the Methane Oversaturation Paradox in an Oxic Freshwater Lake, Environ Microbiol, 19, 1–41,
879 https://doi.org/10.1111/1462-2920.13747, 2018.

880 Wanninkhof, R.: Relationship between wind speed and gas exchange over the ocean, J Geophys Res, 97, 7373–7382,
881 https://doi.org/10.1029/92JC00188, 1992.

882 Weber, T., Wiseman, N. A., and Kock, A.: Global ocean methane emissions dominated by shallow coastal waters, Nat
883 Commun, 10, 1–10, https://doi.org/10.1038/s41467-019-12541-7, 2019.

884 Wiesenburg, D. A. and Guinasso, N. L.: Equilibrium Solubilities of Methane, Carbon Monoxide, and Hydrogen in Water and
885 Sea Water, American Chemical Society, 24, 356–360, 1979.

886   Worden, A.: Picoeukaryote diversity in coastal waters of the Pacific Ocean, Aquatic microbial ecology, 43, 165–175,
887   https://doi.org/doi:10.3354/ame043165, 2006.

888   Ye, W. W., Wang, X. L., Zhang, X.-H., and Zhang, G.-L.: Methane production in oxic seawater of the western North Pacific
889   and its marginal seas, Limnol Oceanogr, 65, 1–14, https://doi.org/10.1002/lno.11457, 2020.

890   Zhang, Y. and Xie, H.: Photomineralization and photomethanification of dissolved organic matter in Saguenay River surface
891   water, Biogeosciences, 12, 6823–6836, https://doi.org/10.5194/bg-12-6823-2015, 2015.

892   Zhao, L., Lin, L.-Z., Chen, M.-Y., Teng, W.-K., Zheng, L.-L., Peng, L., Lv, J., Brand, J. J., Hu, C.-X., Han, B.-P., Song, L.-
893   R., and Shu, W.-S.: The widespread capability of methylphosphonate utilization in filamentous cyanobacteria and its
894   ecological significance, Water Res, 217, 1–11, https://doi.org/10.1016/j.watres.2022.118385, 2022.

895